CHAPTER 3

Visual Perception of the Moving Object

3.1 Introduction

The visual system enables humans to see and observe the events happing in the environment by converting the electromagnetic waves (belonging to a specific frequency range, also known as the visible spectrum) into electrochemical signals (neuronal spiking) and processing them to extract useful information. The process of extracting and organizing information about the surroundings through the visual system is known as visual perception. Visual perception profoundly affects the interaction between a person and her surroundings. From driving a car on a busy highway or playing sports, the visual perception of the moving object is crucial for survival in the natural environment. Modulation or alteration of the perception of the moving stimuli could have appreciable consequences and can affect the quality of life. Therefore, it is vital to understand the underlying neuronal dynamics and anatomical correlates along with the quantifiable model of perception of the moving object.

In the case of a moving object, the position or spatial location of the object changes with time. Therefore, the visual perception of a moving object involves visual-spatial perception, as well as time perception. The process of perceiving a moving object starts with light from the visual field (surroundings) entering the eye and projecting on the retina. The photosensitive cells of the retina convert the light into neural signals, which transmit through the optic nerve to the brain regions. These neuronal signals are projected into the cerebral neuropil forming the retinotopic map, where the relationship between the adjacent location in

the visual field is maintained in terms of nearby neuronal activation (Rosa, 2002). Retinotopic maps are isomorphic representations of the outside world based on information sensed by the retinal system, where the spatiotemporal neuronal activity represents the spatiotemporal movement of the object in the physical space (visual field) (Strasburger, 2022). Retinal images are represented non-linearly on the retinotopic map and have been analyzed by Schwartz (Schwartz, 1980). The retinotopic maps exist in several brain regions, for example, the primary visual cortex (V1) (Bordier et al., 2015), lateral occipital cortex (Larsson and Heeger, 2006), and cerebellum (van Es et al., 2019). High-resolution fMRI imaging enables experimental observation of human retinotopic maps (Olman et al., 2010; Wandell and Winawer, 2011). Retinotopic mapping of the visual field is the initial stage of the processing of the visual perception functions such as motion (Huk et al., 2001), object recognition (Grill-Spector et al., 1998), and color (Engel et al., 1997). The retinotopic map belongs to a broad category of the topographic map, a fundamental neuroanatomical feature in the cerebral cortex of humans and other primates (Bourne and Rosa, 2006; Hartig et al., 2017). We will refer to 'retinotopic map' as 'retinotopic space' for linguistic convenience.

Visual motion perception has been studied to discover underlying neural mechanisms over the years (Albright and Stoner, 1995; Derrington et al., 2004; Nishida et al., 2018). Various experiments have been carried out to find the anatomical and physiological basis of the perception of the moving object using the techniques such as functional magnetic resonance imaging and transcranial magnetic stimulation (Antal et al., 2004; Herrington et al., 2007; Laycock et al., 2007; Tadin et al., 2011). In addition, theoretical explorations addressing the different aspects of motion perception are available, namely, the Reichardt detector for motion detection (van Santen and Sperling, 1985) and the spatiotemporal energy approach (Adelson

and Bergen, 1985). Further work has been done to explore the dominant brain regions active while perceiving a moving object, and to provide theoretical elucidations. Nevertheless, very few studies have addressed the alteration of perception of the moving object and several investigations focused mainly on the perceived speed of the moving object, for example, Mashour found that the perceived speed and actual speed are related to each other by a power law (Mashour, 1981). Algom and Cohen-Raz also reported similar results in another study (Algom and Cohen-Raz, 1984). Therefore, as far as we know, an integrative global mathematical and theoretical framework for the alterations in the perception of a moving object is yet to be readily formalized, specially from a causality perspective.

In this study, we quantified and provided a mathematical model of how the speed of the moving object modifies the visual-spatial perception and time perception while the subject observes the moving object. The changes in the position of the object occur in time-wise order and indicate a temporal causality relationship between the position of the object. We have taken the constancy of temporal causality in the retinotopic space and perceptual space, then find out the relationship or transformation between spatiotemporal coordinates of the moving object represented in the retinotopic space and perceptual space. Here, perceptual space is the subjective experience of the physical space and represents the geometry of the perception. Thereafter, we will apply our mathematical model to different experimental settings to predict results and compare them with actually observed results to validate the outcomes of our investigation. After validation, we will delineate and identify the anatomical regions where the aforesaid perceptual transformation occurs, and experimental verification will be performed by neuroimaging investigations, namely diffusion MRI-based tractography studies. Furthermore, we will formulate a mathematical framework to model the neuronal-level

biochemical mechanism responsible for the modification of visual-spatial perception and time perception, based on neurotransmitter interaction and dynamics from a biochemical perspective.

3.2. Our Mathematical Analysis

In this section, we will formulate the geometrical representation of the moving object in the retinotopic space and its projection onto perceptual space, presuming the invariance of the temporal causality. We will derive a transformation matrix (Z) that consolidates the coordinate transformation from the retinotopic space to the perceptual space while the object changes its position with time. Then, we will show the translation of the transformation equations to the neural systems and demarcate their utilization in the practical scenario.

3.2.1 Geometrical Representation of Moving Object:

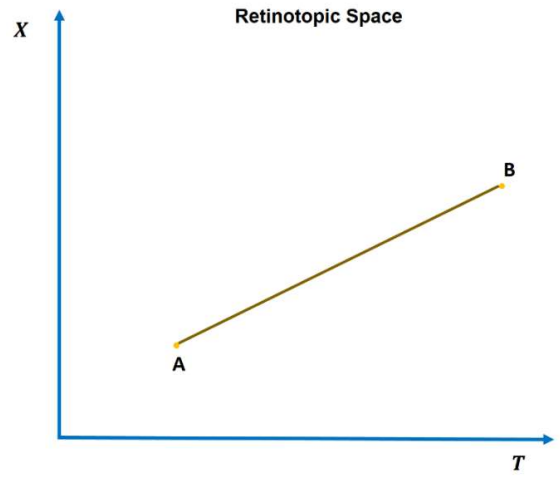

Figure 3.1. Changes in spatial position of the moving object with time in the retinotopic map.

Suppose that the position of an object in the visual field varies with time, such that the change of position with time (speed) is constant. Curve AB in Figure 3.1 represents the spatiotemporal activation of the neural tissue in the retinotopic map due to the changes in the position of the moving object with time (T). Curve AB is a straight line because of the constant speed of the moving object. Every point on the curve AB belongs to the instantaneous neural activation in the retinotopic space corresponding to the instantaneous position of the moving object. We assume that position varies along a single spatial dimension for mathematical convenience. Points A and B in Figure 3.1 denote the start and end of the projection of a moving object on the human observer's retinotopic space.

Let us take a random point R between points A and B in retinotopic space [Figure 3.2(a)]. Every point on curve AB appearing before point R in temporal order has a temporal causal connection with point R. Points A and R of retinotopic space [Figure 3.2(a)] are projected in perceptual space as points A_p and R_p [Figure 3.2(b)], respectively, under the assumption of the invariance of the temporal causality. Therefore, points A_p and R_p in perceptual space also have a causal relationship. In Figure 3.2(b), T* and X^* represent time and position of the object in the perceptual space, respectively.

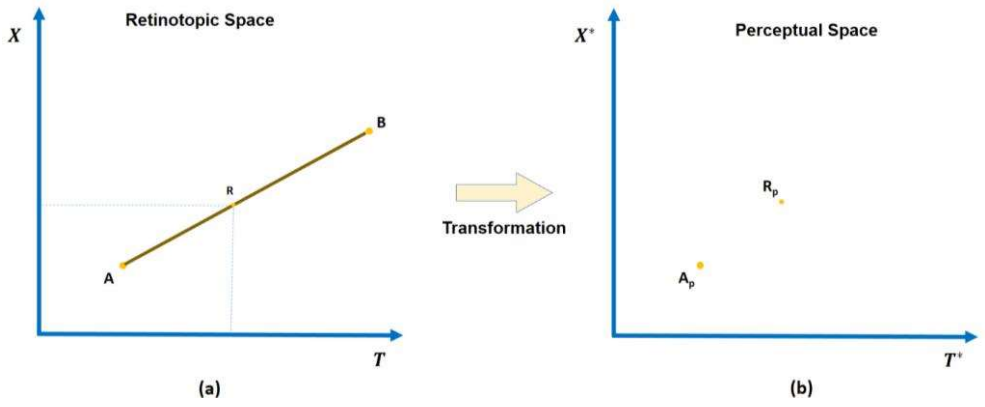

Figure 3.2. Transformation of the representation of the moving object from retinotopic space to perceptual space.

3.2.2 Mapping Coordinate Transformations Between Retinotopic Space and Perceptual Space:

Suppose that in Figure 3.2(a), the coordinates of points R and A are (*t,x*) and (0,0), respectively. As points A and B mark the start and end of the movement of the object in the retinotopic space, the transformation of points A and B in perceptual space should have the same coordinates. An example can explain this: if somebody is watching a ball thrown in the air, the ball's starting and ending position in the retinotopic and perceptual space will be the same. However, anything in between may get modified. Hence the coordinate of point A_p in the perceptual space can be taken to be the same as A, i.e. (0,0), and we assume the coordinate of point R_p in the perceptual space as (t*,x*). (However, under ideal conditions, we expect the coordinates of the points R_p and R to be the same so that the observer perceives the moving object without any modifications.) For generalization, we can presume that the difference in coordinates of points A_p and R_p in the perceptual space is a function of the difference in coordinates of points A and R in retinotopic space. (Equations 3.1a and 3.1b)

$$x^* - 0 = g(t - 0, x - 0)$$
$$x^* = g(t, x) \tag{3.1a}$$
$$t^* - 0 = f(t - 0, x - 0)$$
$$t^* = f(t, x) \tag{3.1b}$$

In Equations 3.1a and 3.1b, the terms *f* and *g* are two functions whose formulations we will pursue later. Likewise, the coordinates of A and R can be mathematically calculated from the coordinates of A_p and R_p under the premises of symmetry between retinotopic and perceptual space.

Therefore:

$$x = g(t^*, x^*) \tag{3.2a}$$

$$t = f(t^*, x^*) \tag{3.2b}$$

Even if point A does not lie on origin, Equations 3.1 and 3.2 must hold. If the coordinates of point A are (x_0, t_0). Then rewriting equations 3.1 and 3.2,

$$x^* - x_0 = g(t - t_0, x - x_0) \tag{3.3a}$$

$$t^* - t_0 = f(t - t_0, x - x_0) \tag{3.3b}$$

$$x - x_0 = g(t^* - t_0, x^* - x_0) \tag{3.4a}$$

$$t - t_0 = f(t^* - t_0, x^* - x_0) \tag{3.4b}$$

Partial differentiation of Equation 3.1a with respect to **x:**

$$\frac{\delta x^*}{\delta x} = \frac{\delta g(t,x)}{\delta x} \tag{3.5}$$

Partial differentiation of equation 3.3a with respect to **x:**

$$\frac{\delta x^*}{\delta x} = \frac{\delta g(t - t_0, x - x_0)}{\delta x} \tag{3.6}$$

From Equations 3.5 and 3.6:

$$\frac{\delta g(t,x)}{\delta x}|_{\{t_0,x_0\}} = \frac{\delta g(t - t_0, x - x_0)}{\delta x}\ |_{\{t_0,x_0\}}$$

$$\frac{\delta g(t,x)}{\delta x}|_{\{t_0,x_0\}} = \frac{\delta g(t - t_0, x - x_0)}{\delta (x - x_0)}\ |_{\{t_0,x_0\}}$$

$$\frac{\delta g(t,x)}{\delta x}|_{\{t_0,x_0\}} = \frac{\delta g(t,x)}{\delta x}\ |_{\{0,0\}} \tag{3.7}$$

Likewise, we can derive from Equation 3.1 – Equation 3.4, the following expressions:

$$\frac{\delta g(t,x)}{\delta t}|_{\{t_0,x_0\}} = \frac{\delta g(t,x)}{\delta t}\ |_{\{0,0\}} \tag{3.8}$$

$$\frac{\delta h(t,x)}{\delta x}|_{\{t_0,x_0\}} = \frac{\delta h(t,x)}{\delta x}\ |_{\{0,0\}} \tag{3.9}$$

$$\frac{\delta h(t,x)}{\delta t}|_{\{t_0,x_0\}} = \frac{\delta h(t,x)}{\delta t}\ |_{\{0,0\}} \tag{3.10}$$

3.2.3 Coordinate Transformation Matrix:

It is evident from Equations 3.7, 3.8, 3.9, and 3.10 that functions *g* and *h* are linear functions of *x* and *t* because the differentiation of functions *g* and *h* is the same at the origin or any arbitrary point (t_0,x_0), which is possible only for a straight line and thus Equations 3.1 and 3.2 becomes:

$$x^* = A.x + B.t \tag{3.11a}$$

$$t^* = C.x + D.t \tag{3.11b}$$

$$x = A.x^* + B.t^* \tag{3.12a}$$

$$t = C.x^* + D.t^* \tag{3.12b}$$

where A, B, C, and D are unknown coefficients in the above Equations 3.11 and 3.12. In the subsequent mathematical analysis, we will derive mathematical expressions for A, B, C, and D.

Let us represent Equations 3.11 and 3.12 in matrix form:

$$\begin{bmatrix} x^* \\ t^* \end{bmatrix} = \begin{bmatrix} A & B \\ C & D \end{bmatrix} \begin{bmatrix} x \\ t \end{bmatrix}$$

$$X^* = Z * X \tag{3.13}$$

$$\begin{bmatrix} x \\ t \end{bmatrix} = \begin{bmatrix} A & B \\ C & D \end{bmatrix} \begin{bmatrix} x^* \\ t^* \end{bmatrix}$$

$$X = Z * X^* \tag{3.14}$$

where $X = \begin{bmatrix} x \\ t \end{bmatrix}$, $X^* = \begin{bmatrix} x^* \\ t^* \end{bmatrix}$ and $Z = \begin{bmatrix} A & B \\ C & D \end{bmatrix}$

In Equations 3.13 and 3.14, Z is a transformation matrix that denotes the coordinates transformation from the retinotopic to the perceptual space. From Equations 3.13 and 3.14, $Z = Z^{-1}$

$$Z = \begin{bmatrix} A & B \\ C & D \end{bmatrix} \tag{3.15}$$

$$Z^{-1} = \frac{1}{BC - AD} \begin{bmatrix} -D & B \\ C & -A \end{bmatrix}$$

For the simplest case, $BC - AD = 1$

$$Z^{-1} = \begin{bmatrix} -D & B \\ C & -A \end{bmatrix} \tag{3.16}$$

By comparison of Equations 3.15 and 3.16, $D = -A$.

Since $BC - AD = 1$. By putting $D = -A$, we get: $BC + A^2 = 1 \quad \Rightarrow \quad A = \pm\sqrt{1 - BC}$

Therefore:

$$Z = \begin{bmatrix} \pm\sqrt{1 - BC} & B \\ C & \mp\sqrt{1 - BC} \end{bmatrix} \tag{3.17}$$

3.2.4 Generalization of Coordinate Transformation Matrix:

In the retinotopic space, the position of the object changes with time, whose rate of change with time can be obtained by putting $x^* = 0$ in Equation 3.11a under the assumption that the rate of change of position with time is constant:

$$0 = A.x + B.t$$

$$\frac{x}{t} = -\frac{B}{A}$$

Let P is the rate of change of position of the moving object in the retinotopic space (i.e., speed):

Then:

$$P = \frac{x}{t} = -\frac{B}{A}$$

$$P = -\frac{B}{\pm\sqrt{1 - BC}}$$

$$\pm\sqrt{1 - BC} = -\frac{B}{P} \tag{3.18}$$

$$C = \frac{1}{B} - \frac{B}{P^2} \tag{3.19}$$

Putting values from Equations 3.18 and 3.19 into Equation 3.17:

$$Z = \begin{bmatrix} -\frac{B}{P} & B \\ \frac{1}{B} - \frac{B}{P^2} & \frac{B}{P} \end{bmatrix} \tag{3.20}$$

Retinotopic maps exist in multiple brain regions. For example, it is present in the primary visual cortex (V1), the cerebellum, and the lateral occipital cortex (Hagler and Sereno, 2006; Larsson and Heeger, 2006; van Es et al., 2019). Let us take two retinotopic maps (t_1 and

t_2), such that the relationship between coordinates of the retinotopic map (t_1), another retinotopic map (t_2), and perceptual space (m) as per our preceding formulation (equation 1 to 20) is as follows (equation 21 to 23), where X^{t1}, $X^{t2,}$ and X^m are the column matrices whose components are the spatiotemporal coordinates of the moving object in the t_1 retinotopic map, t_2 retinotopic map and perceptual space (m) respectively and; Z_1, Z_2 and Z_3 are transformation matrices representing the coordinate transformation.

Relationship between retinotopic maps t_1 and t_2:

$$X^{t2} = Z_1 * X^{t1} \tag{3.21}$$

Relationship between retinotopic map t_2 and Perceptual Space (m):

$$X^m = Z_2 * X^{t2} \tag{3.22}$$

Relationship between retinotopic map t_1 and Perceptual Space (m):

$$X^m = Z_3 * X^{t1} \tag{3.23}$$

3.2.5 Relationship between Spatial Coordinates in Perceptual Space and Retinotopic Space

By comparing the previous three equations (Equations 3.21 to 3.23), we obtained the following:

$$Z_3 = Z_2 * Z_1$$

Applying the transformation matrix Z given in Equation 3.20:

$$\begin{bmatrix} -\frac{B_3}{P_3} & B_3 \\ \frac{1}{B_3} - \frac{B_3}{{P_3}^2} & \frac{B_3}{P_3} \end{bmatrix} = \begin{bmatrix} -\frac{B_2}{P_2} & B_2 \\ \frac{1}{B_2} - \frac{B_2}{{P_2}^2} & \frac{B_2}{P_2} \end{bmatrix} * \begin{bmatrix} -\frac{B_1}{P_1} & B_1 \\ \frac{1}{B_1} - \frac{B_1}{{P_1}^2} & \frac{B_1}{P_1} \end{bmatrix}$$

After matrix multiplication, we obtained the following four equations:

$$-\frac{B_3}{P_3} = \frac{B_1 B_2}{P_1 P_2} + \frac{B_2}{B_1} - \frac{B_1 B_2}{P_1^2} \tag{3.24}$$

$$B_3 = -\frac{B_1 B_2}{P_2} + \frac{B_1 B_2}{P_1} \tag{3.25}$$

$$\frac{1}{B_3} - \frac{B_3}{P_3^2} = -\frac{B_1}{P_1 B_2} + \frac{B_1 B_2}{P_1 P_2^2} + \frac{B_2}{B_1 P_2} - \frac{B_1 B_2}{P_1^2 P_2} \tag{3.26}$$

$$\frac{B_3}{P_3} = \frac{B_1}{B_2} - \frac{B_1 B_2}{P_2^2} + \frac{B_1 B_2}{P_1 P_2} \tag{3.27}$$

Addition of Equations 3.24 and 3.27 gives us:

$$B_1 B_2 \left(\frac{1}{P_1 P_2} + \frac{1}{B_1^2} - \frac{1}{P_1^2}\right) - B_1 B_2 \left(\frac{1}{B_2^2} - \frac{1}{P_2^2} + \frac{1}{P_1 P_2}\right) = 0$$

i.e.
$$B_1 B_2 \left(\frac{1}{P_1 P_2} + \frac{1}{B_1^2} - \frac{1}{P_1^2} - \frac{1}{B_2^2} + \frac{1}{P_2^2} - \frac{1}{P_1 P_2}\right) = 0$$

$$\frac{1}{B_1^2} - \frac{1}{P_1^2} = \frac{1}{B_2^2} - \frac{1}{P_2^2} \tag{3.28}$$

Hence:

$$\left(\frac{1}{B_1^2} - \frac{1}{P_1^2}\right)^2 = \left(\frac{1}{B_2^2} - \frac{1}{P_2^2}\right)^2 \tag{3.29}$$

From Equation 3.26, we have:

$$B_3 \left(\frac{1}{B_3^2} - \frac{1}{P_3^2}\right) = -\frac{B_1 B_2}{P_1}\left(\frac{1}{B_2^2} - \frac{1}{P_2^2}\right) + \frac{B_1 B_2}{P_2}\left(\frac{1}{B_1^2} - \frac{1}{P_1^2}\right) \tag{3.30}$$

Likewise from Equation 3.28, we get:

$$B_3\left(\frac{1}{B_3^2}-\frac{1}{P_3^2}\right)=\left(\frac{1}{B_1^2}-\frac{1}{P_1^2}\right)\left(-\frac{B_1B_2}{P_1}+\frac{B_1B_2}{P_2}\right) \tag{3.31}$$

Taking the square of Equation 3.31 on both sides, we arrive at:

$$B_3{}^2\left(\frac{1}{B_3^2}-\frac{1}{P_3^2}\right)^2=\left(\frac{1}{B_1^2}-\frac{1}{P_1^2}\right)^2\left(-\frac{B_1B_2}{P_1}+\frac{B_1B_2}{P_2}\right)^2 \tag{3.31}$$

Now putting the value of the B_3 from Equation 3.25 into Equation 3.31, we get:

$$\left(\frac{1}{B_3^2}-\frac{1}{P_3^2}\right)^2=\left(\frac{1}{B_1^2}-\frac{1}{P_1^2}\right)^2$$

Therefore:

$$\left(\frac{1}{B_1^2}-\frac{1}{P_1^2}\right)^2=\left(\frac{1}{B_2^2}-\frac{1}{P_2^2}\right)^2=\left(\frac{1}{B_3^2}-\frac{1}{P_3^2}\right)^2 \tag{3.32}$$

In Equation 3.32, the squared term (with the same mathematical arrangement and equivalent variables) is equal in different cases, showing that this particular term is invariant in different situations. Therefore, let us donate Equation 3.32 for the general situation of any space (such as perceptual space, cerebral retinotopic space, or cerebellar retinotopic space) in Equation 3.33, as follows:

$$\left(\frac{1}{B^2}-\frac{1}{P^2}\right)=-\frac{1}{k^2} \tag{3.33}$$

In Equation 3.33, *k* can be considered as a fidelity parameter denoting the invariance across different representational spaces (such as: perceptual space, cerebral retinotopic space, or cerebellar retinotopic space).

By putting the value of B from Equation 3.33 into Equation 3.28, we get:

$$Z = \begin{bmatrix} \frac{-1}{\sqrt{1-\left(\frac{P}{k}\right)^2}} & \frac{P}{\sqrt{1-\left(\frac{P}{k}\right)^2}} \\ \frac{-\frac{P}{k^2}}{\sqrt{1-\left(\frac{P}{k}\right)^2}} & \frac{1}{\sqrt{1-\left(\frac{P}{k}\right)^2}} \end{bmatrix} \quad 3.34$$

Now putting the value of the transformation matrix Z from Equation 3.34 into Equation 3.21:

$$\begin{bmatrix} x^* \\ t^* \end{bmatrix} = \begin{bmatrix} \frac{-1}{\sqrt{1-\left(\frac{P}{k}\right)^2}} & \frac{P}{\sqrt{1-\left(\frac{P}{k}\right)^2}} \\ \frac{-\frac{P}{k^2}}{\sqrt{1-\left(\frac{P}{k}\right)^2}} & \frac{1}{\sqrt{1-\left(\frac{P}{k}\right)^2}} \end{bmatrix} * \begin{bmatrix} x \\ t \end{bmatrix} \quad 3.35$$

Now, in Equations 3.11 and 3.12, the transformation of coordinates from retinotopic to perceptual space or vice versa is the same and occurs when spatial dimensions x and x^* point towards opposite directions. To make them unidirectional, we put $x^* = -x^*$ in Equation 3.35. We get the following:

$$\begin{bmatrix} x^* \\ t^* \end{bmatrix} = \begin{bmatrix} \frac{-1}{\sqrt{1-\left(\frac{P}{k}\right)^2}} & \frac{P}{\sqrt{1-\left(\frac{P}{k}\right)^2}} \\ \frac{-\frac{P}{k^2}}{\sqrt{1-\left(\frac{P}{k}\right)^2}} & \frac{1}{\sqrt{1-\left(\frac{P}{k}\right)^2}} \end{bmatrix} * \begin{bmatrix} x \\ t \end{bmatrix}$$

Hence, the relationship between the coordinates of retinotopic and perceptual space is:

$$x^* = \frac{x - Pt}{\sqrt{1 - \left(\frac{P}{k}\right)^2}} \quad \& \quad t^* = \frac{t - \frac{Px}{k^2}}{\sqrt{1 - \left(\frac{P}{k}\right)^2}} \tag{3.36}$$

3.2.6 Translation to the Neural System.

The moving object in the visual field (physical space) is projected on the retina, and then the position of the moving object is mapped from the retinal surface in the retinotopic space. In the transformation equation (Equation 3.36), x and t are physical coordinates in the retinotopic space. However, the physical size of the visual field (where the object is moving in external space) differs from the physical size of the cortical tissues (where retinotopic space is situated). Figure 3.3 illustrates the cortical magnification factor (CMF) (Slotnick et al., 2001), which defines the cortical tissue allotted (in mm) for one degree of the visual angle subtended at the eye. CMF gives the ratio of the size of the neuronal tissue (z) activated due to the movement of an object in the visual field, subtending a particular visual angle (θ) (Swearer, 2011). The visual field projected around the fovea obtains more neural tissue compared to peripheral regions, as shown by decreasing values of the CMF in the peripheral region of the retina (Cowey and Rolls, 1974).

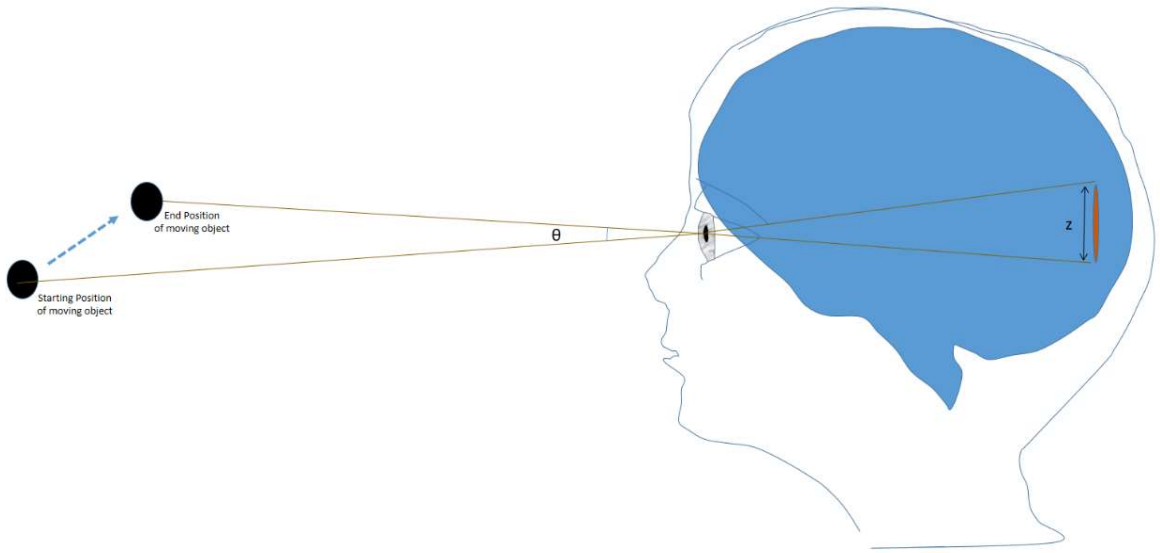

Figure 3.3: The cortical magnification factor denotes the cortical tissue involved in the retinotopic representation of the given size of the visual field. The cortical magnification factor is the ratio of the size of the cortical tissue (z) and the visual angle subtended on the eye (θ).

On the contrary, x^* represents the perceived extent of the position of the external event in the perceptual space. To make x^* compatible with the physical size of the moving object, it is necessary to re-map x^* to enable comparison of x^* value with the physical value of the position of the moving object. Therefore, applying the cortical magnification factor in a reverse way will modify the x^* to become compatible with the physical scale of the visual field. Suppose that γ represents the cortical magnification factor function (which quantitatively shows the mapping of the position of the moving object from the visual field to the retinotopic map) and *w* is the physical position of the moving object. Then the relationship between θ, x, x^* and ɳ is given by the following Equation 3.37, where ɳ represents the perception of the position of the moving object. The inverse function γ^{-1} represent the brain's mechanism to make neural activation compatible with the physical extent of external events.

$$x = \gamma\,(w) \qquad \text{and} \qquad \eta = \gamma^{-1}(x^*) \tag{3.37}$$

In Equation 3.37, γ and γ^{-1} are the mathematical functions, and the term inside the parenthesis or round brackets is input to the function, while the γ^{-1} is an inverse function of the mathematical function γ. Our formulation of the perception of a moving object is shown in Figure 3.4, where the transformation equations (Equation 3.36) were derived in the previous section.

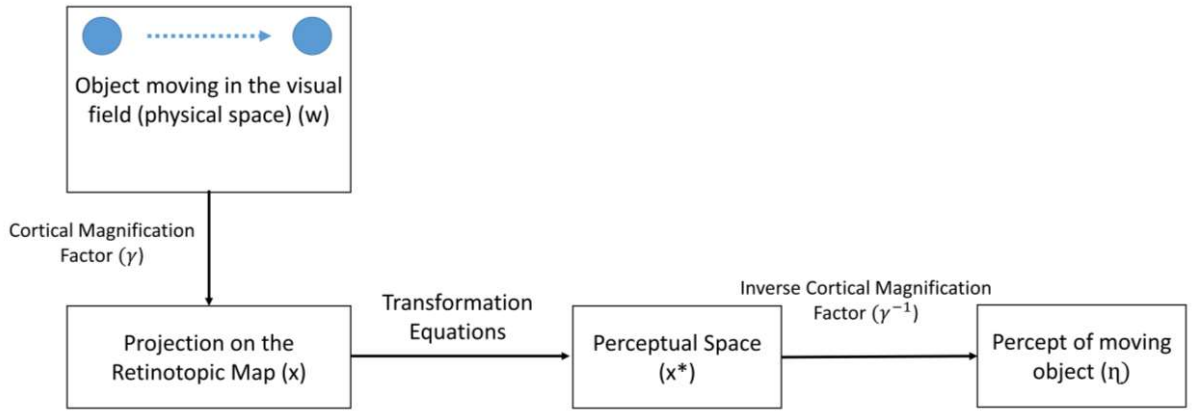

Figure 3.4: Our formulation of perception of a moving object: The moving object is projected on the retinotopic map through the retinal surface and follows the cortical magnification factor for mapping from the visual field to the retinotopic map. Then, transformation equations relate the spatiotemporal coordinate of the moving object in the retinotopic and perceptual space. After that, on applying the inverse cortical magnification factor provides the coordinates of the perceived moving object at the scale of physical space.

Apart from this, in the transformation equations (Equation 3.36), *P* is the rate of the change of the position of the moving object in retinotopic space (i.e., speed). At the same time, *k* (fidelity parameter) transpires to be a constant. As highlighted by Equations 3.32 and 3.33,

the fidelity parameter is constant irrespective of the frame of references. Because neural signals are responsible for transferring information between retinotopic space and perceptual space, the fidelity parameter might be related to the neuronal signals.

3.3. Empirical Validation of the Mathematical Analysis

The transformation equations (Equation 3.36) show that the spatiotemporal coordinates of the moving object in perceptual space can be different from the spatiotemporal coordinates in the retinotopic space and thus indicates that the perception of a moving object may deviate from the physical reality. Now we will analyze two experiments using our formulation of the perception of the moving stimuli (Figure 3.4). Then we will theoretically predict the experimental outcomes and compare them with actual results to validate our theoretical formulation.

3.3.1 Methods

3.3.1.1 Moving Arc

A luminous arc was formed on a wheel having a diameter of 61 cm. The length of the arc and radial distance of the arc from the center was 13 cm and 20.7 cm, respectively. A flat black box with a horizontal line facing the subject is situated before the center of the wheel. The length of this horizontal line can vary through the rolling shutter as desired by the subject. The presence of the black box did not affect the visibility of the path of the rotating arc. Distance between the subject and the rotating wheel varied between 2 to 4 feet. Different speeds of 0, 0.5, 0.7, 1, and 1.3 revolutions per second were used to rotate the wheel. Speed could not be increased beyond 1.3 revolutions per second as subjects could not follow the arc and saw a complete circle. A total of 12 subjects participated in the experiment. Two groups were formed

out of the subjects; for one group, the speed varied from lowest to highest, and for the other one, vice-versa. Subjects vary the length of the stationery line to match it with the length of the moving arc (Ansbacher, 1944). Figure 3.5 illustrates the experimental setup.

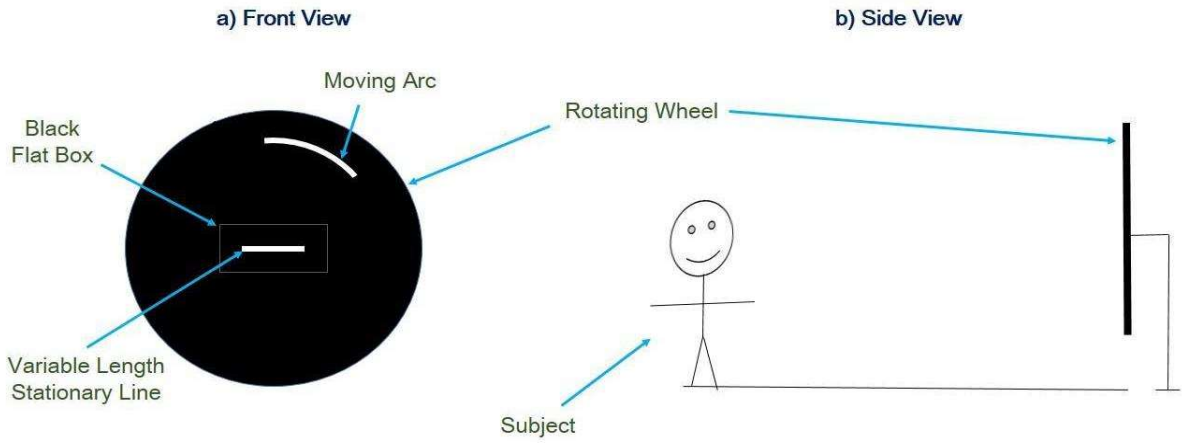

Figure 3.5 Experimental setup for measuring the perceived length of a moving arc at different speeds.

During the experiment, subjects need to fixate on the middle of the horizontal line, which coincides with the center of the circle traced by the moving arc, and judge the length of the moving arc at the different rotational speeds of the wheel. Subjects varied the length of the stationary line to make it subjectively equal to the length of the moving arc.

3.3.1.2 Temporal Perception

Matching and reproduction methods were used to measure the perceived time period for eight subjects. Participants fixated at 6.6 degrees above the Gabor patch while the chin rest restrained any head movement. Vertical Gabor patches with six degrees radius displayed on the CRT monitor act as stimuli and are placed at 57 centimeters from the participants. Sinusoidal luminance modulation drifting left or right of the stationary Gaussian contrast

envelope in the Vertical Gabor patch was used as moving stimuli. In contrast, a vertical Gabor patch without any luminance modulation was used as stationary stimuli. Two methods were used to measure perceived time while perceiving moving stimuli (Kaneko and Murakami, 2009):

- In the matching method, the moving stimuli was displayed for a fixed time duration, followed by stationary stimuli whose duration was varied to make, so that the subjects assessed it subjectively equal to the moving stimuli's duration.
- In the reproduction method, the moving stimuli was displayed on the screen for some period, after which subjects reproduced the perceived duration by pressing a switch.

3.3.2 Results

3.3.2.1 Perception of a Moving Arc

The perceived length of the moving arc was measured by Ansbacher using the experiment setup explained in section 3.3.1.1 (Ansbacher, 1944). Figure 3.6 shows the experimental measurement of the variation in the perceived length as the rotation speed of the moving arc varies from 0 to 1.3 revolutions per second, obtained by Ansbacher. As shown in Figure 3.6, reduction in the perceived length indicates the alteration of visual perception due to a change in the speed of the arc.

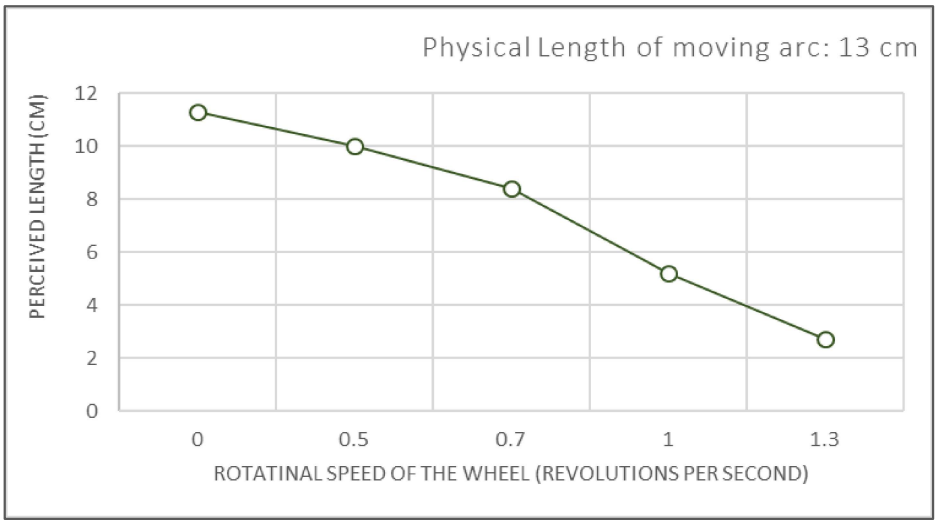

Figure 3.6. Alteration in the perceived length of the moving arc at different rotational speeds of the arc.

Next, we analyzed the experimental data using our mathematical framework. We obtained the relationship between the length of the moving arc at retinotopic space and perceptual space. The length of the moving arc at retinotopic space (L) is as follows (where x_1 and x_2 are spatial coordinates of the start and end point of the moving arc at the retinotopic space on a particular moment, t=T_0):

$$L = x_2 - x_1 \tag{3.38a}$$

Then, applying the transformation equation (Equation 3.36), the length of the moving arc at perceptual space (L^*):

$$L^* = x_2^* - x_1^* = \frac{x_2 - PT_0}{\sqrt{1 - \left(\frac{P}{k}\right)^2}} - \frac{x_1 - PT_0}{\sqrt{1 - \left(\frac{P}{k}\right)^2}}$$

$$L^* = \frac{L}{\sqrt{1 - \left(\frac{P}{k}\right)^2}} \tag{3.38b}$$

In Equation 3.38b, P is the speed of the moving arc in the retinotopic space. We find out the length of the moving arc at retinotopic space (L) using the physical length of the arc and the length of the moving arc at perceptual space (L*) using experimental observation shown in Figure 3.6, as well as the speed (P), by applying the cortical magnification factor (CMF). Therefore, we calculated CMF for the moving arc (physical length: 0.13 meters) based on experimental observations from different studies (Rovamo and Virsu, 1979; Tolhurst and Ling, 1988; Horton and Hoyt, 1991; Duncan and Boynton, 2003; Larsson and Heeger, 2006; Schira et al., 2007). Since CMF decreases for the peripheral visual field. Thus, we found out the average value of the tissue allocated per degree of the visual field (CMF) used by the observer to make a judgment.

In this experiment, the circular path followed by the moving arc subtended an angle of 23.4 degrees on the retina. Therefore, the angular distance from the fovea was 11.7 degrees. The calculated cortical magnification factor (γ) was 9.55 mm of neural tissue per degree of the visual field, represented as γ in Figure 3.4. Although the arc followed a circular path while subjects make length judgments, the circle will be mapped to a line in retinotopic space due to logarithmic mapping (Schwartz, 1980). The rotational velocity of the moving arc was converted into linear velocity, followed by applying γ to find the value of P (the speed of the arc in the retinotopic space).

Since we have experimental observations about L, L^* and P. Furthermore, we calculted k (fidelity parameter) by putting these values in Equation 3.38b. As per our earlier analysis (Equations 3.32 and 3.33), the value of k (fidelity parameter) should be constant regardless of the speed of the moving arc.

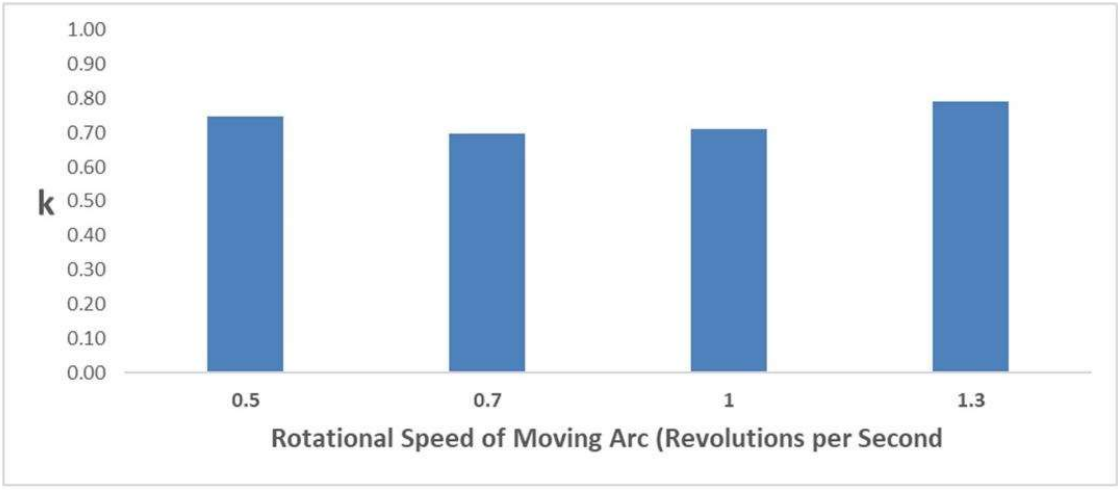

Figure 3.7 Constancy of the fidelity parameter k, while the rotational speed of moving arc changes. This constancy validates the theoretical prediction of our mathematical model. (Statistical goodness-of-fit test satisfied, $p > 0.99$).

We obtained the fidelity parameter (k) for different rotational speeds of the moving arc, and the results are shown in Figure 3.7. As evident in Figure 3.7, the value of the fidelity parameter (k) is almost constant irrespective of the speed of the moving arc in the retinotopic space. From Equation 3.38(b), we find that as the P's value approach toward the fidelity parameter (k), the subject's underestimation of the arc's length $(L - L^*)$ increases. From Figure 3.7, we see that the fidelity parameter (k) has a very small coefficient of variation (~ 5%) with an average value of 0.74 and can be taken as a constant. The chi-square (χ^2) goodness of fit test is also satisfied (p>0.99). The constant value of the fidelity parameter across different

observation conditions supports our mathematical prediction. This constancy of the fidelity parameter ensures full faithfulness and correspondence between the different representations of the moving object in different spaces (i.e. perceptual space, cerebral retinotopic space, or cerebellar retinotopic space).

3.3.2.2 Perception of Time

Over the years, various researchers consistently observed temporal overestimation when the external stimulus moves compared to the stationary stimulus (brown, 1995; Mate et al., 2009; Karşilar et al., 2018). Now we will predict the observations of a similar experiment using our model and compare it with the actual results to validate our model. Kaneko and Murakami performed a similar experiment measuring the perceived time period during stationary and moving stimuli. The perceived time was measured using two experimental procedures: in the first procedure, the matching method was used in which the duration of the stationary stimuli varied till it was perceived as equal to the duration of the moving stimulus. The second procedure incorporates the reproduction method in which subjects reproduce the perceived duration of the moving stimulus by pressing the switch (Kaneko and Murakami, 2009). The ratio of perceived time and actual time was used to quantify the perceptual changes in the subjects, termed as the ratio of overestimation.

Using transformation equations (Equation 3.36), we derived the mathematical equation (Equation 3.39), which provides the time-interval transformation from retinotopic (Δt) to perceptual space (Δt^*) at a particular spatial coordinate ($x=X_0$).

$$\Delta t^* = t_1^* - t_2^* = \frac{t_1 - \frac{PX_0}{k^2}}{\sqrt{1 - \left(\frac{P}{k}\right)^2}} - \frac{t_2 - \frac{PX_0}{k^2}}{\sqrt{1 - \left(\frac{P}{k}\right)^2}}$$

$$\Delta t^* = \frac{t_1 - t_2}{\sqrt{1 - \left(\frac{P}{k}\right)^2}}$$

$$\Delta t^* = \frac{\Delta t}{\sqrt{1 - \left(\frac{P}{k}\right)^2}} \tag{3.39}$$

Now, to found out the speed of the moving stimulus at the retinotopic space, we calculated the CMF for the current experiment. In this experiment, subjects fixate their eyes 6.6 degrees above the Gabor patch center, whose diameter is 12 degrees. Therefore, 12.6 degrees of the visual field undergo movement. Using the same procedure used in section 3.3.2, we obtained the average cortical magnification factor equal to 9.51 mm of the neural tissue per degree of the visual field.

We used the value of $k = 0.74$, obtained after analyzing the perception of the moving arc experiment in the previous section 3.3.2.1 After that, we calculated the perceived time interval at different speeds using Equation 3.39 and plotted this data along with corresponding experimental measurements for comparison, shown in Figures 3.8 and 3.9. Then we performed the chi-square (χ^2) goodness-of-fit test to test the congruence of our mathematical prediction compared to actual observations. We obtained $p > 0.99$ for both experiments, which indicates that our mathematical model is well corroborated.

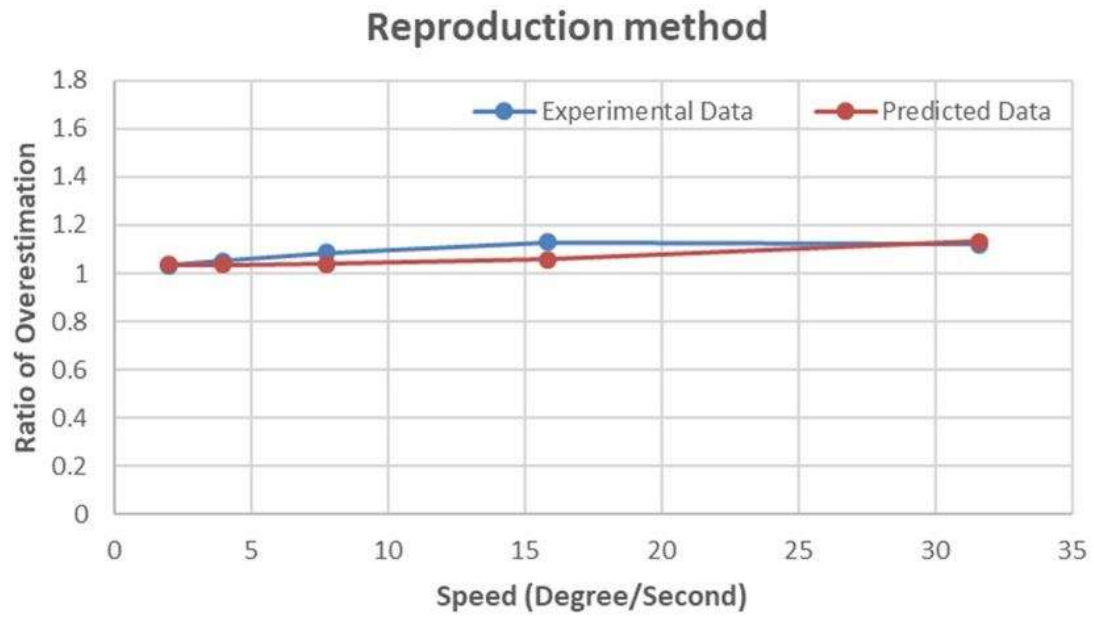

Figure 3.8. Experimental observations of the reproduction method (second experiment) validates the theoretical prediction of our mathematical model. (Statistical goodness-of-fit test satisfied, $p > 0.99$).

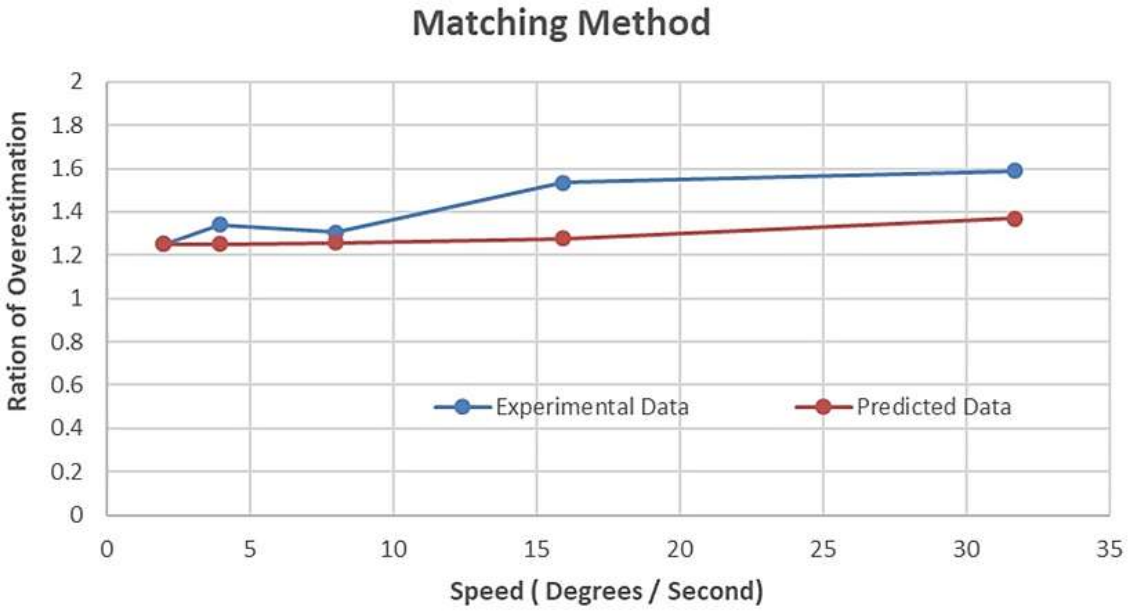

Figure 3.9. Experimental observations of the matching method (first experiment) validates the theoretical prediction of our mathematical model. (Statistical goodness-of-fit test satisfied, $p > 0.99$).

3.4 Anatomical Correlates

3.4.1 Conceptual Observations

In the previous section (3.3), we validated our model based on empirical evidences and showed that our mathematical formulation reliably describes the ongoing perception phenomenon. In this section, we will examine the anatomical region in the brain, which implements the coordinate transformation equation (Equation 3.36).

In the transformation equation (Equation 3.36):

- The position in perceptual space (x^*) is a function of spatial (x) and temporal (t) coordinates in the retinotopic space.
- The time in perceptual space (t^*) is a function of spatial (x) and temporal (t) coordinates in the retinotopic space.

This indicates that the position in perceptual space (x^*) depends partly on time (t) in the retinotopic space, in addition to the spatial information in the retinotopic map (x). Similarly, time in perceptual space (t^*) depends partly on position (x) in the retinotopic space, in addition to the temporal information in the perceptual space (t). These observations are counterintuitive as when an object is not moving (P=0), the visual-spatial perception of the object depends on the only spatial position, and temporal perception depends only on the time-information. Nevertheless, the motion of the object causes two different information streams (spatial and temporal) along the motion perception pathways to interact with each other. In other words, temporal information (t) also takes part in the perception of spatial information (x^*) due to this interaction process (in addition to spatial information (x)). Similarly, spatial information (x) also takes part in the perception of time (t^*) due to this interaction process (in addition to

temporal information(t)). This interaction process modulates the perception of spatial position and time, which was also observed in the experiments discussed in the previous section (3.3.2).

Now we come to the interaction of the space-time coordinates during motion. Suppose that a pendulum is moving in a fronto-parallel plane of an observer. The observer perceives the oscillating movement of the pendulum in a plane from her naked eyes. However, when the same observer views after placing a neutral density filter in front of one eye, she perceives the pendulum's movement in an elliptical orbit, making the pendulum appear to move close to her (rightward swing of the pendulum) and then far from her (leftward swing of the pendulum). This phenomenon is known as the Pulfrich illusion, named after its discoverer Carl Pulfrich who was ironically blind in one eye (Petzold and Pitz, 2009). A neutral density filter introduces a time delay in processing the retinal image (Wilson and Anstis, 1969; Reynaud and Hess, 2017), and during perception, time delay affects spatial perception. The magnitude of the perceived depth depends on the change in the pendulum's position with time (i.e., speed) (Qian and Andersen, 1997). In contrast with the perception of the moving object, the interaction between spatial and time dimensions is experimentally observable in the Pulfritch phenomenon (Anzai et al., 2001).

Now we come to the neuroanatomical correlate of the interaction between the spatial and temporal information during the perception of the moving object. Several experimental studies (Beckers and Zeki, 1995; Laycock et al., 2007; D'Alfonso et al., 2013) have observed that the middle temporal visual area (V5) is active during perceiving moving stimuli. Similarly, during the Pulfrich illusion, the middle temporal visual area (V5) is active, as observed experimentally (Spang and Morgan, 2008). Hence we may conclude that during the process of visual motion

perception, which involves interaction between time and spatial information, the middle temporal visual area (V5) is the anatomical locus of interaction.

3.4.2 Diffusion MRI Tractography Experiment

3.4.2.1 Methods

(i) *Subject A*: Diffusion-weighted images were acquired on a 3T Philips Achieva scanner at National Brain Research Centre, Manesar, India, using the HARDI schema (128 direction, b-value: 2000 sec/mm^2). The human MRI scanning procedure was approved by the Institutional Human Ethics Committee of the National Brain Research Centre, and informed consent was taken. In-plane resolution and slice thickness were 2 mm. FSL eddy was used to correct for eddy current distortion through the integrated interface in DSI Studio ("Chen" release). The diffusion MRI data were rotated to align with the AC-PC line. After motion correction, deterministic fiber tracking was performed using DSI Studio using the following tracking parameters: fractional anisotropic threshold: 0.04162, angular threshold: 75 degrees, step size: 0.1 mm, and total seeds: 1000000. We performed this analysis pipeline for one normal subject (Gender: Male, Age: 24 years).

(ii) *Subject B*: Scans were acquired on a 7T Siemens MAGNETOM machine at Maastricht University, Netherlands. Approval was given by the Ethics Committee of the Faculty for Psychology and Neuroscience at Maastricht University, and informed consent was obtained. Diffusion-weighted MRI images were scanned using multi-band diffusion-weighted spin-echo EPI protocol with the following parameters: b-values = 1000, 2000, and 3000 s/mm^2, FOV = 200 x 200 mm with partial Fourier 6/8, 132 slices, 1.05 mm isotropic voxel size, TR = 7080 ms, TE = 75.6 ms, 66 directions and 11 additional b = 0

volumes for every b-value (Sitek et al., 2019). The susceptibility artifact was estimated using reversed phase-encoding b0 by TOPUP from the Tiny FSL package (http://github.com/frankyeh/TinyFSL), a re-compiled version of FSL TOPUP (FMRIB, Oxford) with multi-thread support. FSL eddy was used to correct for eddy current distortion. After preprocessing the MRI image, we used DSI Studio software (http://dsi-studio.labsolver.org) for deterministic tractography using the diffusion tensor imaging technique (Basser et al., 1994). We used Brainnetome Atlas to locate the region of interest (ROI) (Fan et al., 2016). The tracking parameter was fractional anisotropy threshold 0.06, angular threshold of 65 degrees, step size 0.1mm, and 500000 seeds. We performed this analysis pipeline for one normal subject (Gender: Female, Age: 27 years).

(iii) *Subject 1 to 30*: We randomly selected 30 cognitive normal subjects from the Open Access Series of Imaging Studies (OASIS) human brain scan platform (LaMontagne et al., 2019) for diffusion weighted MRI acquisition. The scans had 64 diffusion sampling directions and an in-plane resolution of 2.5mm. Ethics committee approval was given by the Knight Alzheimer Disease Research Center at Washington University, St. Louis, USA. The diffusion MRI scans were rotated to align with the AC-PC line. The accuracy of b-table orientation was examined by comparing fiber orientations with those of a population-averaged template (Yeh et al., 2018). The diffusion tensor metrics were calculated using DWI (diffusion weighted imaging) with b-value lower than 1750 s/mm^2. A deterministic fiber tracking algorithm (Yeh et al., 2013) was used. After preprocessing, we used the following tracking parameters in DSI Studio (http://dsistudio.labsolver.org)

to find the neural tracts: anisotropy threshold was 0.04162, the angular threshold was 75 degrees, the step size was 0.1 mm, and a total of 100000 seeds were placed.

3.4.2.2 Results

Although we may conclude by analyzing earlier studies that mentioned middle temporal area V5 of the visual brain takes part in the spatial-time interaction, perception is a complex process involving several cortical areas. Therefore, we investigated the anatomical connectivity between the area V5 and brain regions active during visual-spatial and temporal perception by analyzing the diffusion-MRI scans to find the concerned neural tracts. We analyzed earlier literature findings (Andersen et al., 1985; Sakata and Kusunoki, 1992; Harrington et al., 1998; Onoe et al., 2001; Ferrandez et al., 2003; Leon and Shadlen, 2003; Lewis and Miall, 2003; Ivry and Spencer, 2004; Janssen and Shadlen, 2005; Konen and Kastner, 2008; Jazayeri and Shadlen, 2015; Protopapa et al., 2019) which delineated the brain regions responsible for (i) time perception (temporal aspect) and (ii) perception of a position of an object located in the visual field (spatial aspect). Based on the literature analysis, we find the differential brain areas activated during time and visual spatial perception, as mentioned in Table 3.1 below.

Table 3.1. Brain regions active during perception of time and perception of the spatial location of an object.

Perception of Time	**Perception of Spatial Location of object**
Prefrontal Cortex (Brodmann Area 45)	Posterior Parietal Cortex (Brodmann Area 7)
Premotor Cortex (Brodmann Area 4 & 6)	Intraparietal Sulcus
Inferior Parietal Cortex (Brodmann Area 40)	Superior Parietal Lobule
Putamen (Basal Ganglia)	

Then we tracked the neural tracts in each hemisphere between the following brain regions:

- "brain regions active during time perception" and "area V5".
- "brain regions active during visual-spatial perception" and "area V5".
- Area V5 of the left and right hemispheres.

Initially, we performed a tractography experiment for subject A and subject B (please see the section 3.4.2.1 for the method); the results are shown in Figures 3.10 and 3.11. The tractography results indicate that area V5 has anatomical connectivity to brain regions along the time and spatial position information processing streams. Area V5 can act as a conjoint point or interaction center for these two streams. Then, we performed the centrality analysis of the network consisting of the brain regions listed in Table 3.1 as nodes. We constructed the hemisphere-wise networks for visual-spatial and time perception, in which the corresponding brain regions involved in the tractography analysis were nodes. We calculated the centrality parameter for each node which signifies the importance of that node in the information flow or connectivity in the network. Using the DSI studio procedure (http://dsi-studio.labsolver.org), we computed each node's eigenvector centrality and PageRank centrality. Results of the centrality analysis are shown in Tables 3.2 and 3.3, which highlighted that area V5 has the highest centrality in the networks and is the most significant node in the network. Furthermore, our observations showed consonance in our findings from the 3-tesla scanner and 7-tesla scanner.

Table 3.2 Eigenvector centrality and PageRank centrality of the different brain regions as nodes of the network for Subject-A regarding time perception and spatial perception.

Subject A (MRI field: 3T)				
Brain regions active during "Spatial Perception"				
	Eigenvector Centrality (Weighted)		PageRank Centrality (Weighted)	
Brain Regions as nodes	Left Hemisphere	Right Hemisphere	Left Hemisphere	Right Hemisphere
MT / V5	0.5590	0.6577	0.4088	0.3834
Superior Parietal Lobule	0.4103	0.0156	0.1535	0.0366
Posterior Parietal Cortex	0.3505	0.3811	0.2154	0.1897
Intraparietal Sulcus	0.4700	0.6493	0.0688	0.3538
Brain regions active during "Time Perception"				
	Eigenvector Centrality (Weighted)		PageRank Centrality (Weighted)	
Brain Regions as nodes	Left Hemisphere	Right Hemisphere	Left Hemisphere	Right Hemisphere
Prefrontal Cortex	0.1347	0.0752	0.0610	0.0540
Premotor Cortex	0.0933	0.0000	0.0456	0.0268
Inferior Parietal Cortex	0.0413	0.2979	0.0343	0.1576
Putamen (Basal Ganglia)	0.4145	0.0000	0.1680	0.0268
MT / V5	0.6949	0.6985	0.4088	0.3661

Table 3.3 Eigenvector centrality and PageRank centrality of the different brain regions as nodes of the network for Subject B regarding time perception and spatial perception.

Subject B (7T)				
Space Perception				
	Eigenvector Centrality (Weighted)		Pagerank Centrality (Weighted)	
	Left Hemisphere	Right Hemisphere	Left Hemisphere	Right Hemisphere
MT / V5	0.5182	0.6152	0.2683	0.3172
Superior Parietal Lobule	0.2248	0.1850	0.1199	0.1050
Posterior Parietal Cortex	0.5145	0.6119	0.2448	0.3133
Intraparietal Sulcus	0.5181	0.3319	0.2471	0.1594
Time Perception				
	Eigenvector Centrality (Weighted)		Pagerank Centrality (Weighted)	
	Left Hemisphere	Right Hemisphere	Left Hemisphere	Right Hemisphere
Prefrontal Cortex	0.0014	0.0000	0.0211	0.0316
Premotor Cortex	0.0000	0.0147	0.0205	0.0370
Inferior Parietal Cortex	0.0037	0.0000	0.0323	0.0316
Putamen (Basal Ganglia)	0.5629	0.5508	0.2558	0.2520
MT / V5	0.6051	0.6190	0.3292	0.2957

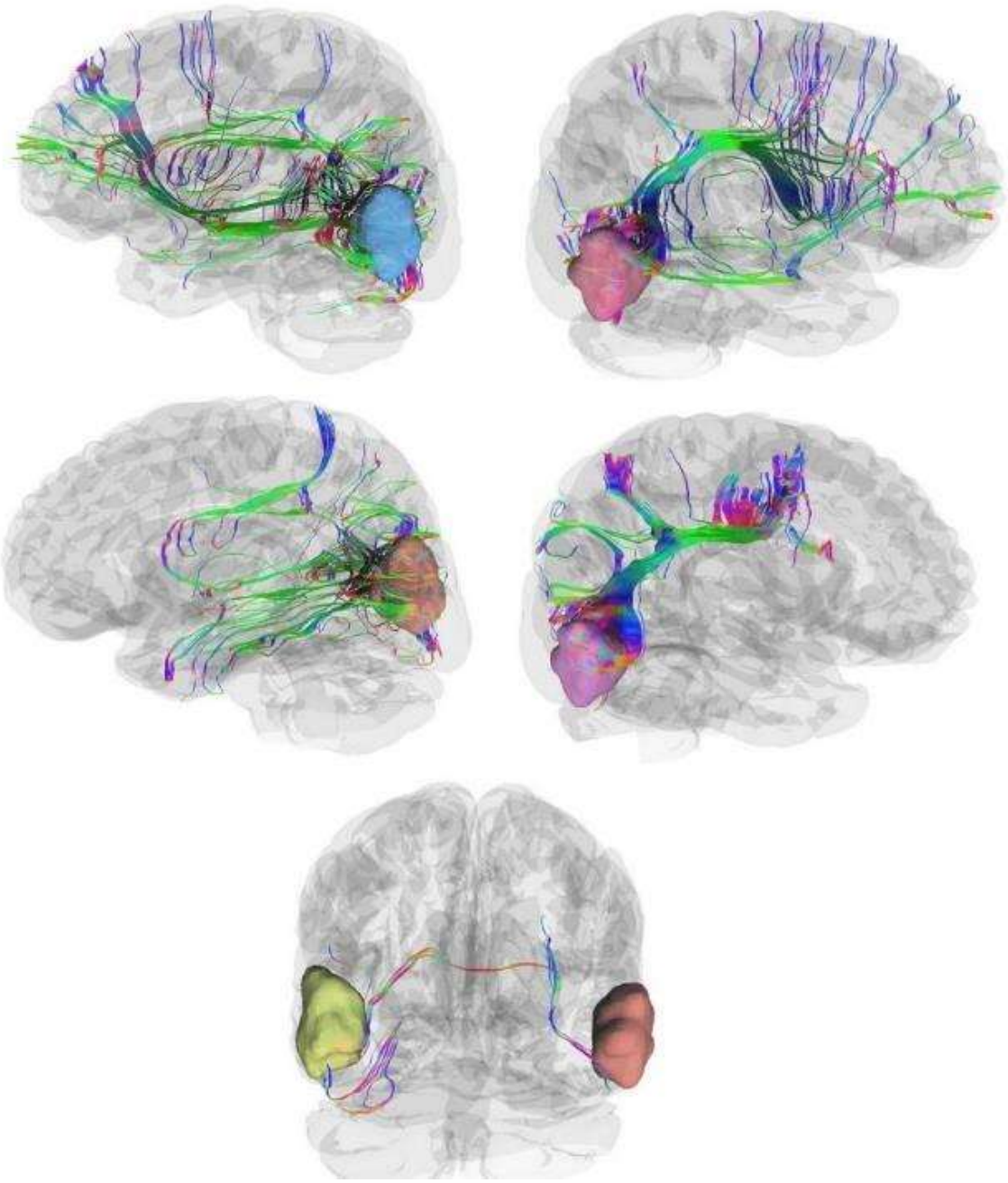

Figure 3.10 Pathways for spatio-temporal interaction (Subject A, MRI 3 tesla scanner). *Upper Row:* Tracts between middle temporal visual area (V5) and brain regions active during time perception. *Middle Row:* Tracts between middle temporal visual area (V5) and brain regions active during spatially locating of an object. *Lower Row:* Tracts between left and right middle temporal visual area (V5). (The brain regions are listed in Table 3.1).

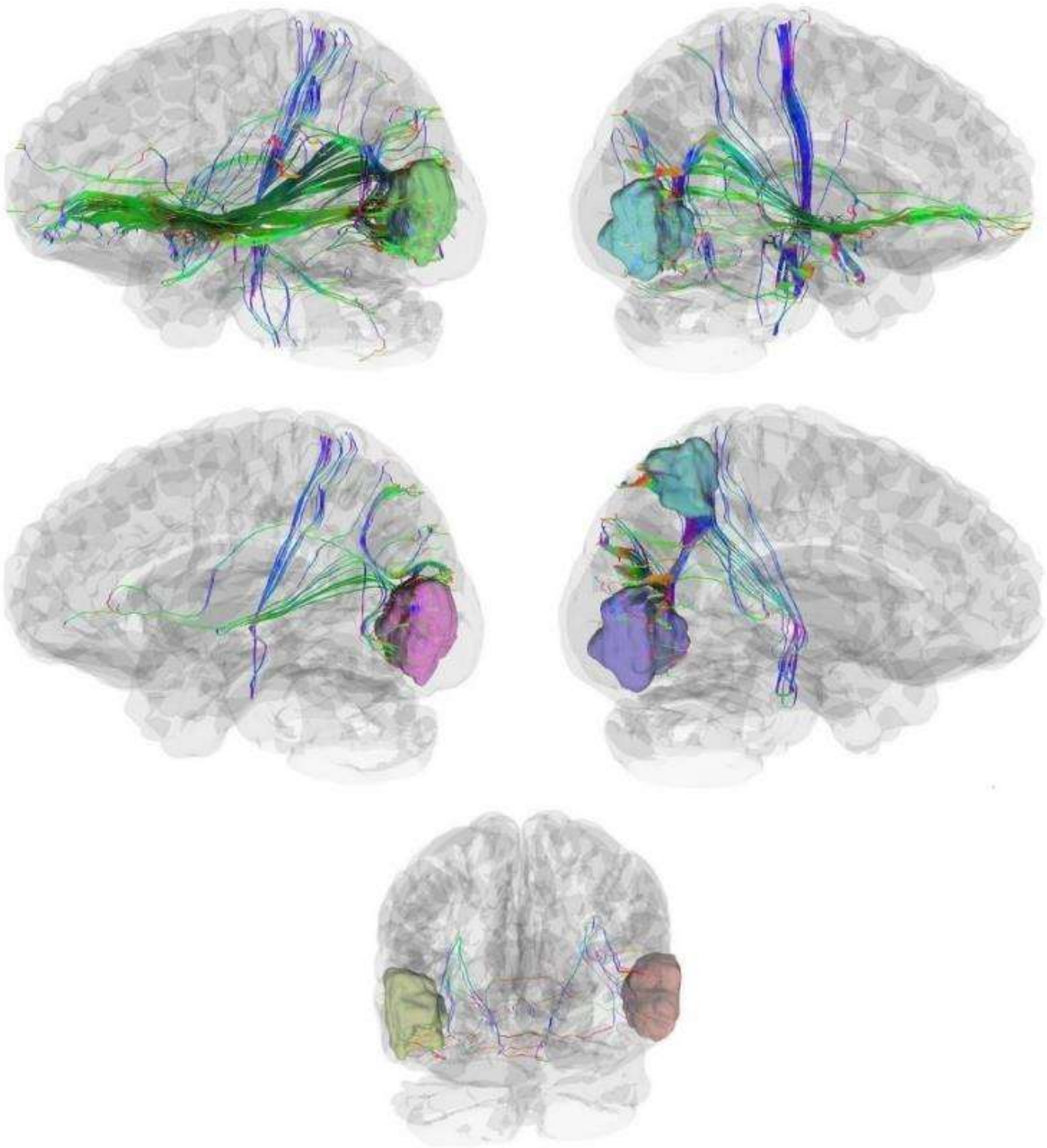

Figure 3.11 Pathways for spatiotemporal interaction (Subject B, MRI 7 tesla scanner): *Upper Row:* Tracts between middle temporal visual area (V5) and brain regions active during time perception. *Middle Row:* Tracts between middle temporal visual area (V5) and brain regions active during spatially locating an object. *Lower Row:* Tracts between left and right middle temporal visual area (V5). (The brain regions are listed in Table 3.1).

Next, we aimed to validate the presense of the neural tracts by analysing the diffusion MRI scans of the 30 subjects (please refer section 3.4.2.1 for the method). We processed the diffusion MRI scans to extract the tracts connecting area V5 with the regions involved in time perception and spatial perception, respectively. The resulting tracts for all 30 participants are presented in Figure 3.12, Figure 3.13, Figure 3.14, and Figure 3.15. The significant parameters associated with tracts are provided in Tables 3.4 and 3.5. The findings from the tractography analysis indicate that for all 30 subjects, the area V5 exhibits anatomical connections with brain regions involved in processing both time information as well as spatial position information. This suggests that the middle temporal area V5 may serve as the interaction point for these two information processing streams.

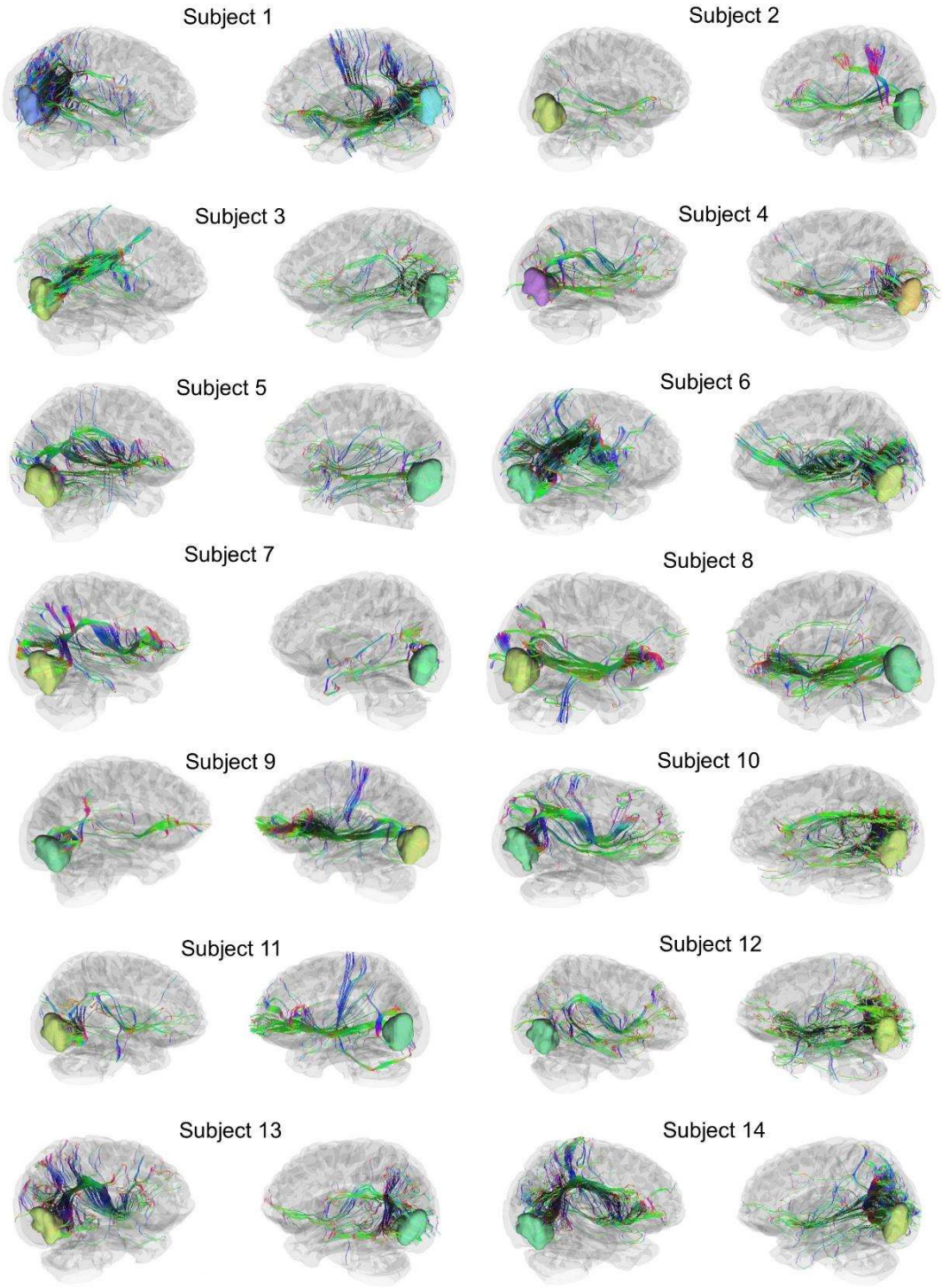

Figure 3.12 Time Perception: Neural tracts between middle temporal visual area (V5) and brain regions active during temporal perception for Subject 1 to Subject 14.

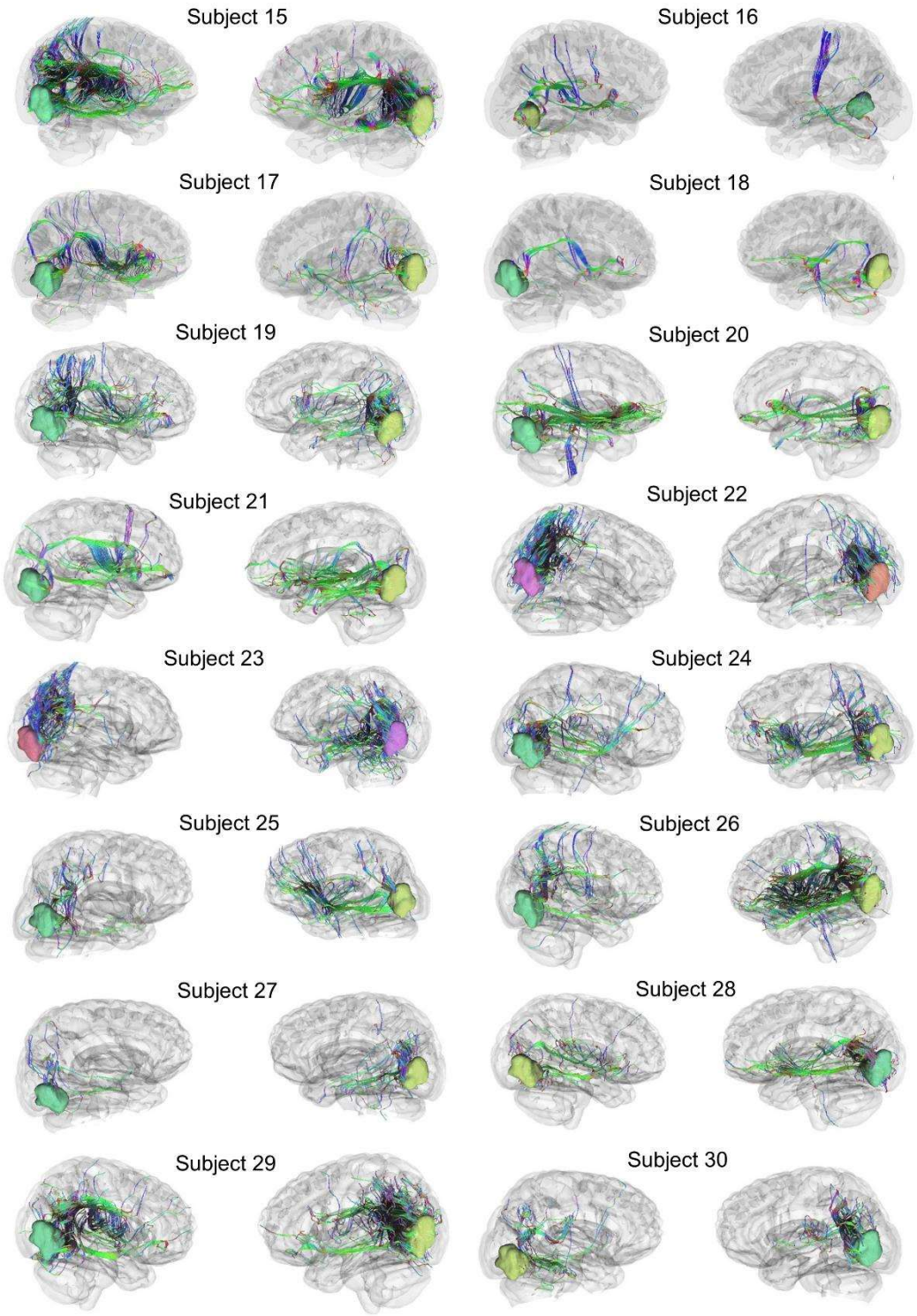

Figure 3.13 Time Perception: Neural tracts between middle temporal visual area (V5) and brain regions active during temporal perception for Subject 15 to Subject 30.

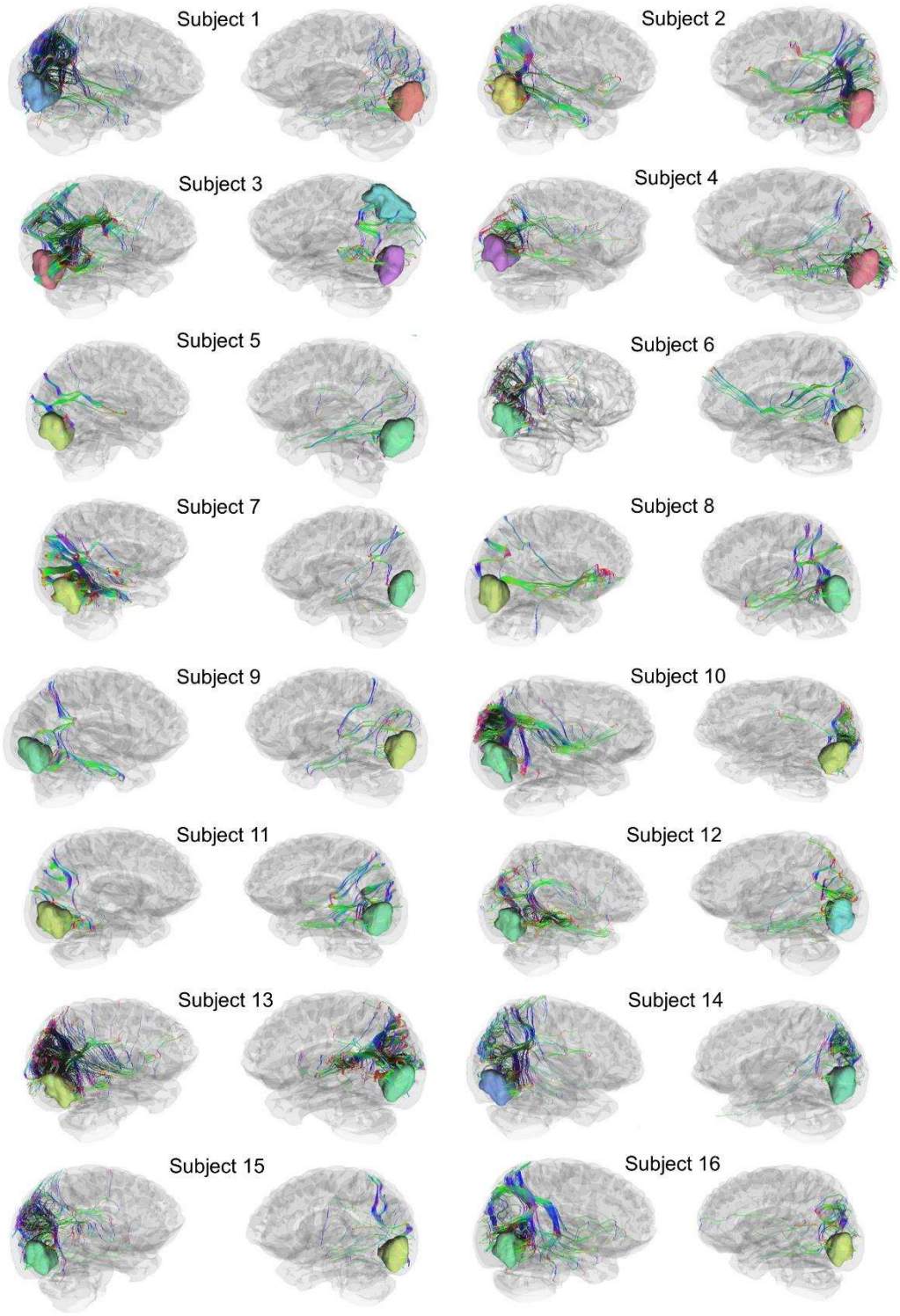

Figure 3.14 Spatial location perception: Neural tracts between middle temporal visual area (V5) and brain regions active during spatially locating an object for subject 1 to subject 16.

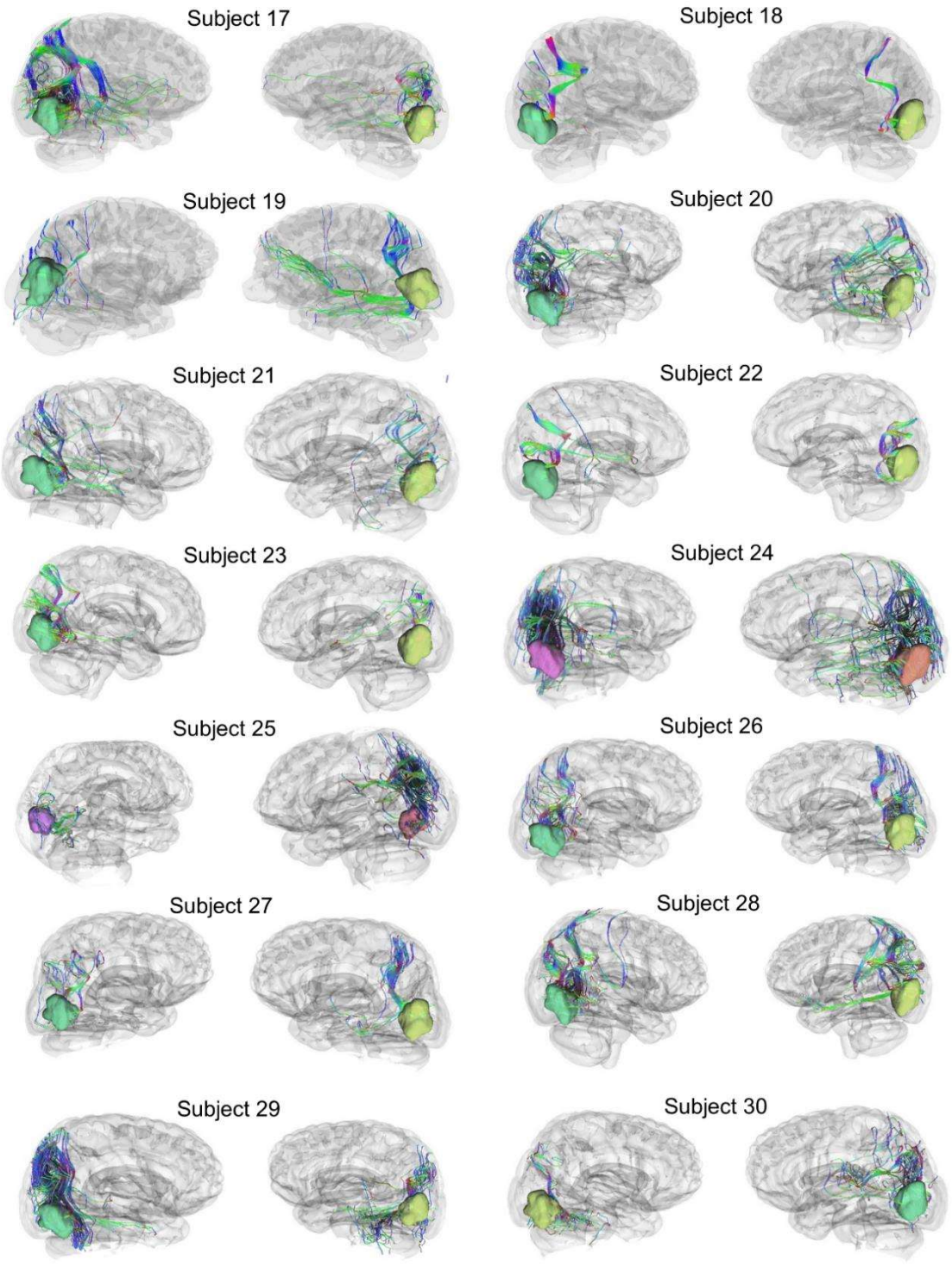

Figure 3.15 Spatial Location Perception: Neural tracts between middle temporal visual area (V5) and brain regions active during spatially locating an object for subject 17 to subject 30.

Table 3.4 Fiber tract parameters related to the neural tracts connecting the area V5 and brain regions active during time perception for subjects 1 to 30.

Parameters	Left Hemisphere	Right Hemisphere
Mean length (mm)	178.7 ± 33.6	187.6 ± 43.7
Fractional Anisotropy	0.3468 ± 0.03	0.3544 ± 0.03
Mean Diffusivity	0.9976 ± 0.12	0.9998 ± 0.12
Axial Diffusivity	1.3500 ± 0.12	1.3579 ± 0.13
Radial Diffusivity	0.8214 ± 0.10	0.8208 ± 0.13

Table 3.5 Fiber tract parameters related to the neural tracts connecting the area V5 and brain regions active during spatially locating an object for subjects 1 to 30.

Parameters	Left Hemisphere	Right Hemisphere
Mean length (mm)	179.9 ± 41.7	173.8 ± 32.5
Fractional Anisotropy	0.3415 ± 0.03	0.3391 ± 0.02
Mean Diffusivity	1.0016 ± 0.11	0.9980 ± 0.11
Axial Diffusivity	1.3410 ± 0.15	1.3333 ± 0.13
Radial Diffusivity	0.8319 ± 0.10	0.8303 ± 0.13

3.5. Proposed Neuronal Level Mechanism

Different experimental studies pointed out the role of different neurotransmitters during the time and visuo-spatial perception. While an object moves in the visual field, perception of time is modulated by Dopamine levels (Liu et al., 2017; Mikhael and Gershman, 2019). Similarly, Acetylcholine modulates the spatial perception of the moving object (Gratton et al., 2017). Therefore, the corresponding biochemical mechanism (of interaction between visual-spatial and temporal information) may be the modulatory effect of Acetylcholine and Dopamine levels on each other.

In the brain tissue, Acetylcholine and Dopamine release can affect each other's concentration due to mutual neuromodulation at the synaptic cleft. Here, we elucidate that a similar mechanism will occur in area V5 of the visual cortex. Muscarinic acetylcholine receptors can regulate dopamine release. However, for instance, in the case of low-frequency stimuli (1 to 10 Hz), Acetylcholine suppresses dopamine release, however, for high-frequency stimuli (> 25 Hz), dopamine release probability increases (Threlfell et al., 2010, 2012). Similarly, dopamine can promote the release of Acetylcholine through D1 receptors while suppressing Acetylcholine release through D2 receptors (Imperato et al., 1993; Abercrombie and DeBoer, 1997; Di Cara et al., 2007; Martorana et al., 2009). It is also known that the Dopamine D1 receptor's density is significantly more than the D2 receptor's density in the visual cortex (Lidow et al., 1991; Mueller et al., 2020). Therefore, dopamine promotes Acetylcholine release, and Acetylcholine through Muscarinic receptors suppresses dopamine release in the area V5 as there is usually low-frequency activity.

To paraphrase, the Dopamine-Acetylcholine interaction will cause changes in dopamine and Acetylcholine concentration with time. We can model interaction in the Lotka-Volterra system, developed for chemical reaction dynamics.

Thereby, we can formulate that

$$\frac{dA}{dt} = mA - \mu AD \tag{3.40}$$

$$\frac{dD}{dt} = -mD + \beta AD \tag{3.41}$$

where:

A = Instantaneous concentration of Acetylcholine at the synaptic cleft ($millimoles$)

D = Instantaneous concentration of Dopamine at the synaptic cleft ($millimoles$)

μ = Density of Dopamine D1 receptor on dendrites ($micromoles\ per\ meter^2$)

β = Density of Acetylcholine Muscarinic receptor on dendrites ($micromoles\ per\ meter^2$)

m = Interaction parameter ($per\ millisecond$) ($0 < m \leq 1$)

We used Runge-Kutta 4th order method to find the numerical solution of Equations 3.40 and 3.41. We calculated the density of Dopamine D1 (μ) and Acetylcholine Muscarinic receptor (β) in the visual cortex using experimental observation from another study (Zilles and Palomero-Gallagher, 2017). We obtained μ = 0.0381 micromoles per meter^2 and β = 0.0996 micromoles per meter^2. Using these values and keeping the interaction parameter (m) equal to 1, we calculated the dopamine and acetylcholine concentration dynamics, as shown in Figure 3.16.

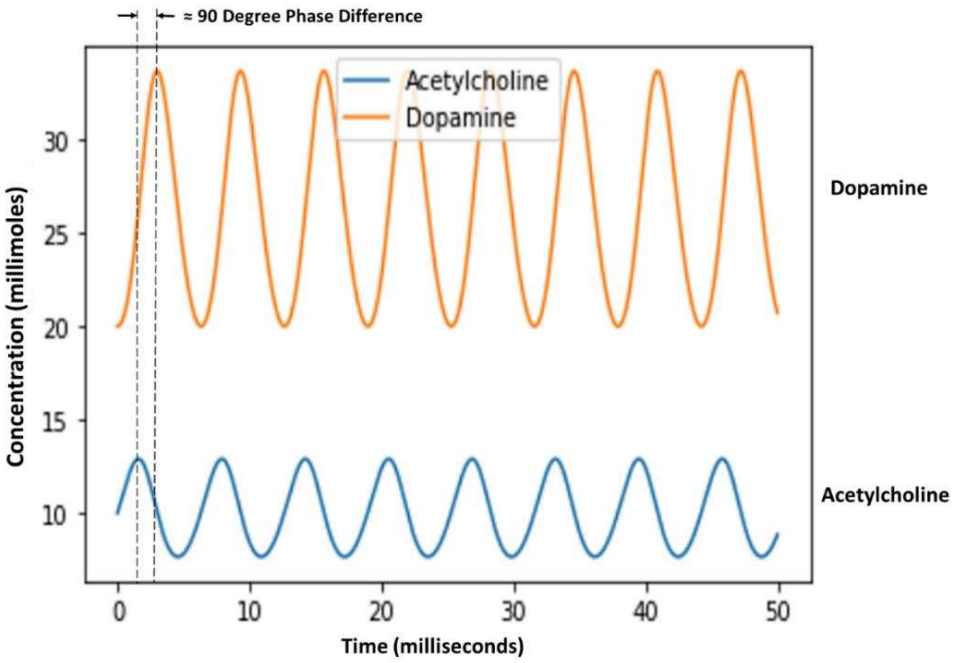

Figure 3.16 Temporal dynamics of acetylcholine concentration and dopamine concentration.

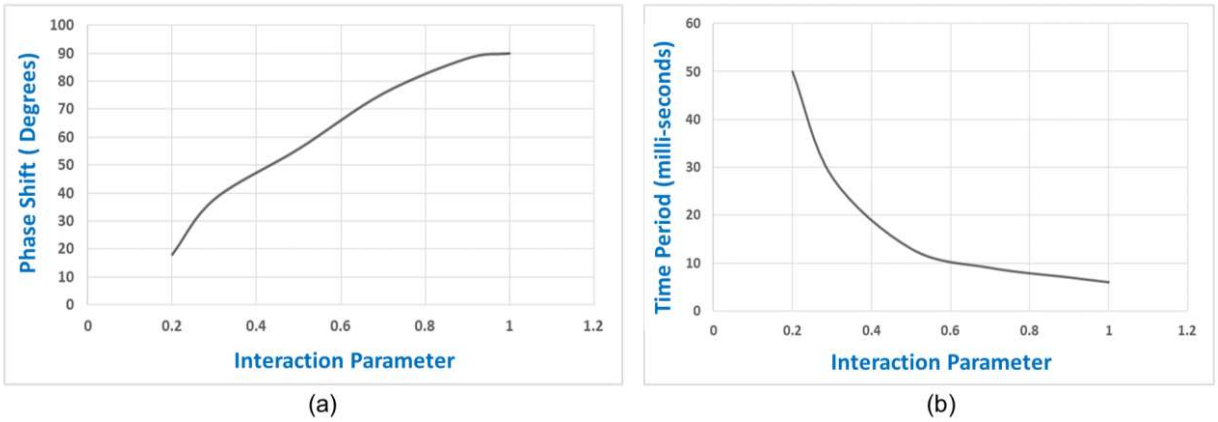

Figure 3.17 (a) Alteration of the phase shift between the oscillatory concentrations of dopamine (or Acetylcholine), while the acetylcholine-dopamine interaction parameter varies. (b) Alteration of the oscillation time period of Acetylcholine (or dopamine), while the acetylcholine-dopamine interaction parameter varies.

As evident from Figure 3.16, the resulting concentrations are oscillatory with an orthogonal phase difference (around 90 degrees) between them. When we gradually increased the interaction parameter (m) from 0 to 1, the phase difference increased with the maximum value of 90 degrees at $m = 1$ (Figure 3.17a). Thus, the interaction parameter affects the phase shift between oscillatory dopamine and acetylcholine concentration, and we can formulate that the interaction parameter (m) signifies the interaction between the time and spatial information streams.

The tilted spatiotemporal receptive field profile of complex neuronal cells in area V5 is tuned to a particular spatiotemporal frequency, resulting in perceiving the equivalent speed (McLean and Palmer, 1989; Perrone and Thiele, 2002; Priebe et al., 2003; Giaschi et al., 2007; Pawar et al., 2019). Therefore, the change in perception of a moving object should result from the alterations in neuronal tuning properties in area V5. As the speed of the moving object varies, the interaction between time and spatial information stream also varies due to changes in the interaction between Dopamine and Acetylcholine. Dopamine and Acetylcholine interact with each other via receptors at dendrites (axon-dendrite synapse), which may modulate the spatiotemporal receptive field of complex cells and change the tuning speed of complex cells. Due to the changes in tuning properties of the complex cells, the perception of the moving object will get modulated.

This dynamic mechanism furnishes a process by which spatial information and temporal information can interact and modulate the perception of the moving object (graphical illustrated in Figure 3.18). Thus, we observed the significance of the axodendritic synapse for spatiotemporal interaction.

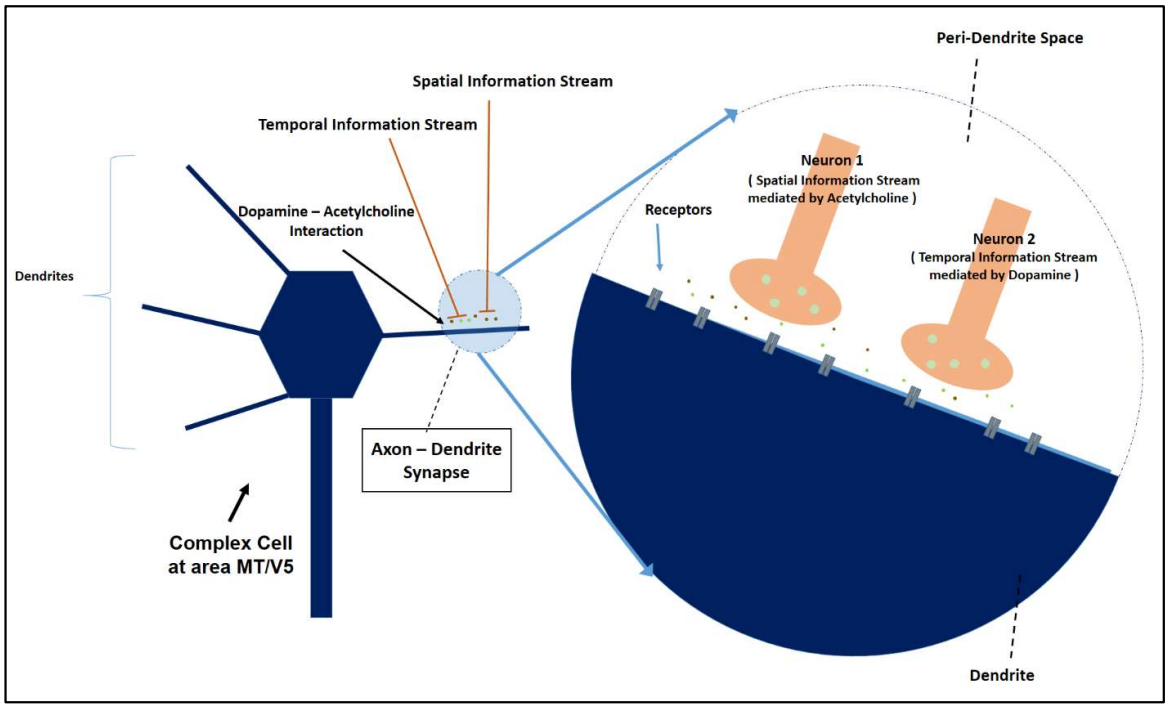

Figure 3.18 Possible biochemical basis of the interaction of the spatial information stream and the temporal information stream during the perception of a moving object, the interaction occurring at the axodendritic synapse.

3.6 Formal Analysis of the Perception of Moving Object

Considering that a spatial position of an object in the visual field is constant, an observer can predict from her perception that the object is static for how much time. Even without any change in the spatial position of the object, the time information stream is present in the brain for time perception. When multiple objects change positions in the visual field at different rates, an observer can perceive that different objects change their positions differently. Therefore, we can take that time, and spatial information streams are represented separately and independently in the brain. However, these two streams interact to link time and

change in spatial position during visual spatiotemporal perception of a moving object. As already mentioned, this integration happens in area V5 of the visual cortex.

Since temporal information and spatial information are independent information streams in the brain, therefore in the vectorial representation, they should be orthogonal to each other. Figure 3.19(a) is the pictorial representation of the spatial ($\vec{S}$) and time vector ($\vec{T}$), because of the orthogonality, the magnitude of the resultant vector ($\vec{S}$) follow Pythagoras's theorem.

$$\vec{S} = \vec{X} + \vec{T} \qquad (3.42(a))$$

$$|S|^2 = |X|^2 + |T|^2 \qquad (3.43(b))$$

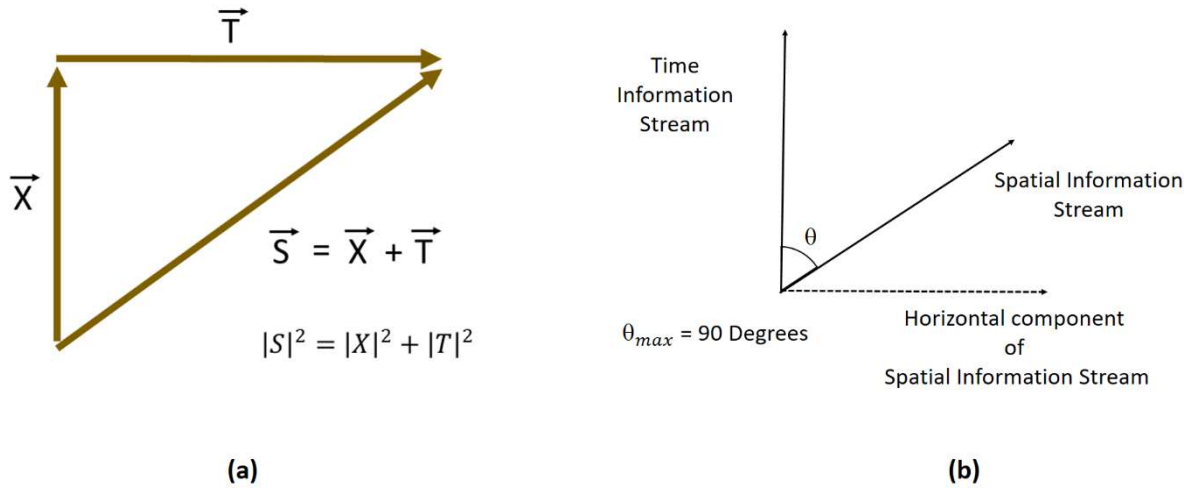

Figure 3.19 (a) Vectorial representation of the interaction between the Spatial information stream (X) and the Time information stream (T). **(b)** Interaction between the orthogonal components of the time information stream and spatial information stream.

$\vec{S}$ is a mathematical synonym with displacement or length and, therefore, the magnitude of $\vec{S}$ should be the equal irrespective of the frame of reference (either retinotopic space or perceptual space). Let's put the constraint that the $|S|^2$ is equal in the retinotopic space and perceptual space.

The object is moving in one spatial dimension, and let us take two random points on the spatiotemporal path of the moving object. Suppose that the coordinates of the two points are (x_1, t_1) and (x_2, t_2) in the retinotopic space. In the perceptual space, corresponding coordinates are (x_1^*, t_1^*) and (x_2^*, t_2^*), respectively. We used Pythagoras's theorem to calculate $\vec{S}$ (vector addition of temporal vector and spatial vector). Putting the constraint that $|S|^2$ is equal in the retinotopic space and perceptual space and take that the: $\vec{X} = \alpha\ \vec{x}$ and $\vec{T} = \beta\ \vec{t}$

In retinotopic space, we have from Equation 3.43b:

$$|X|^2 = \alpha^2(x_2 - x_1)^2 \text{ and } |T|^2 = \beta^2(t_2 - t_1)^2$$

Thus
$$|S|^2 = \alpha^2(x_2 - x_1)^2 + \beta^2(t_2 - t_1)^2 \tag{3.44}$$

Likewise in perceptual space, we have from Equation 3.43b:

$$|X|^2 = \alpha^2(x_2^* - x_1^*)^2 \text{ and } |T|^2 = \beta^2(t_2^* - t_1^*)^2$$

Hence
$$|S|^2 = \alpha^2(x_2^* - x_1^*)^2 + \beta^2(t_2^* - t_1^*)^2 \tag{3.45}$$

Putting values of the x* and t* from Equation 3.36 into Equation 3.45:

$$|S|^2 = \alpha^2 \frac{(x_2 - Pt_2 - x_1 + Pt_1)^2}{1 - \left(\frac{P}{k}\right)^2} + \beta^2 \frac{\left(t_2 - \frac{Px_2}{k^2} - t_1 + \frac{Px_1}{k^2}\right)^2}{1 - \left(\frac{P}{k}\right)^2}$$

$$|S|^2 = \frac{\alpha^2}{1-\left(\frac{P}{k}\right)^2}\left((x_2-x_1)^2 + P^2(t_1-t_2) + 2P(x_2-x_1)(t_1-t_2)\right)$$
$$+\frac{\beta^2}{1-\left(\frac{P}{k}\right)^2}\left((t_2-t_1)^2 + \frac{P^2}{k^4}(x_1-x_2)^2 + \frac{2P}{k^2}(x_2-x_1)(t_1-t_2)\right)$$

$$|S|^2 = \left(\frac{\alpha^2}{1-\left(\frac{P}{k}\right)^2} + \frac{P^2\beta^2/k^4}{1-\left(\frac{P}{k}\right)^2}\right)(x_2-x_1)^2 + \left(\frac{P^2\alpha^2}{1-\left(\frac{P}{k}\right)^2} + \frac{\beta^2}{1-\left(\frac{P}{k}\right)^2}\right)(t_2-t_1)^2 + \left(\frac{2P\alpha^2}{1-\left(\frac{P}{k}\right)^2} + \frac{2P\beta^2/k^2}{1-\left(\frac{P}{k}\right)^2}\right)(x_2-x_1)(t_1-t_2) \quad (3.46)$$

Comparing the terms of $\alpha^2$and β^2 in Equation 3.46 with Equation 3.44, we got the following three equations:

$$\frac{\alpha^2}{1-\left(\frac{P}{k}\right)^2} + \frac{P^2\beta^2/k^4}{1-\left(\frac{P}{k}\right)^2} = \alpha^2 \quad (3.47)$$

$$\frac{P^2\alpha^2}{1-\left(\frac{P}{k}\right)^2} + \frac{\beta^2}{1-\left(\frac{P}{k}\right)^2} = \beta^2 \quad (3.48)$$

$$\frac{2P\alpha^2}{1-\left(\frac{P}{k}\right)^2} + \frac{2P\beta^2/k^2}{1-\left(\frac{P}{k}\right)^2} = 0 \quad (3.49)$$

Simplifying the Equations 3.47, 3.48 or 3.49 yields the same results, i.e. :

$$\alpha^2 = -\frac{\beta^2}{k^2} \quad (3.50)$$

Putting value of β^2 from Equation 3.50 into Equation 3.45, we obtain the following:

$$|S|^2 = \alpha^2(x_2^* - x_1^*)^2 - \alpha^2k^2(t_2^* - t_1^*)^2 \quad (3.51)$$

Now let us take: $x_2^* - x_1^* = x$ and $t_2^* - t_1^* = t$, thereby Equation 3.51 becomes:

$$|S|^2 = \alpha^2 x^2 - \alpha^2 k^2 t^2 \tag{3.52}$$

where α is a scalar. For α =1, we note the equality of retinotopic space (Equation 3.44) and perceptual space (Equation 3.45).

Putting α=1 in Equation 3.52, we arrive at:

$$|S|^2 = x^2 - k^2 t^2 \tag{3.53(a))}$$

Hence: $$\vec{X} = \vec{x} \text{ and } \vec{T} = jk\vec{t} \tag{3.53(b))}$$

where $j = \sqrt{-1}$, j being an imaginary number.

If we analyze the above equations (Equation 3.53a and 3.53b), we can find insight into what happens during the perception of a moving object. $\vec{X}$ and $\vec{T}$ represent temporal and spatial information streams while $\vec{S}$ represent interaction resultant among them. We now recollect that dopamine and Acetylcholine modulate the perception of time and spatial location, respectively. The 90-degree orthogonal phase shift between Dopamine and Acetylcholine oscillatory concentration (shown in Figure 3.16) is mathematically expressed as j $(= \sqrt{-1})$ in Equations 3.53(a) and 3.53(b), showing the interaction of time perception and spatial perception. Moreover, in Figure 3.17(a), phase shift varies with changes in interaction parameter (m). This change in phase shift will result in a variation in interaction level as only the orthogonal components of the spatial vector and time vector will interact, as shown in Figure 3.19b. As the value of phase shift approaches 90 degrees, the magnitude of the horizontal component of the spatial information stream will increase. In consequence, the magnitude of the interaction vector $\vec{S}$ will increase too. Hence, the perception of the moving

object will vary as the interaction parameter varies. Therefore, the value of the interaction parameter is proportional to the speed of the moving object (from earlier analysis, we know that the perception of the moving object varies with the speed of the moving object).

3.7 Discussions

3.7.1 Mathematical Model

The environment from different vantage points is not a static system but a dynamic one. This dynamic nature is observable along the temporal dimension as different events occur in the spatiotemporal arena. Causality defines the framework for assessing the causal or generative relationship between two events. Deducing the causal-effect relationship between events is an innate feature of human cognition. This is such an essential cognitive ability that causal understanding is one of the fundamental differences between human and nonhuman brains (Penn et al., 2008; Stuart-Fox, 2015). In this paper, we formulated a theoretical framework for perceiving a moving object under the invariant representation of temporal causality in the retinotopic space and perceptual space. For this, we represented the change in the position of a moving object with time as the spatiotemporal coordinates in the retinotopic space and perceptual space. Thereby, we could derive transformation equations that explain the transformation of the spatiotemporal coordinates of the moving object from retinotopic space to perceptual space.

In the transformation equation (Equation 3.36), P (speed) quantifies the dynamic nature of the position of the moving object, and the fidelity parameter (k) delineates the possible role of the anatomical characteristics of the brain in the perception. The transformation

equation predicted that the perception of a moving object would vary with speed and was later observed in the moving arc and time perception experiment. Equation 3.33 predicted that the numerical value of the fidelity parameter (k) is constant, which was subsequently verified by analyzing experimental findings of the moving arc experiment using our approach. We calculated the value of the fidelity parameter and showed the value to be robustly constant ($k = 0.74$), as predicted by our theoretical model. The fidelity parameter represents the conformity and correspondence between the different representations of the moving object in different spaces, such as perceptual space, cerebral retinotopic space, and cerebellar retinotopic space. We investigated another experimental study (that measured the perceived time) to validate our mathematical model further. Using the transformation equations and k=0.74 (the value obtained after analyzing the moving arc experiment), we predicted the perceived time, which satisfactorily followed the experimental outcomes (goodness of fit test, p>0.99). Thus, we verified the transformation equation based on the empirical analysis. Our results indicate that the conservation of causality between retinotopic and perceptual spaces shapes the observer's perception of moving object. The novel findings furnish a new dimension to understanding perception by developing an innovative multi-scale mathematical formulation.

3.7.2 Anatomical Correlates

The transformation equation shows that the position of the object at perceptual space (x^*) depends on both position (x) and time (t) at retinotopic space. Similarly, the time at perceptual space (t^*) depends on both position (x) and time (t) at retinotopic space. Thus, we could conclude that at the perceptual space, the time(t) and position(x) information interact during the visual-spatial and temporal perception. However, during the perception of a moving

object, the interaction between the temporal and spatial information is not explicitly observable. But, the interaction between the temporal and spatial information is explicitly observable during the perception of the moving pendulum with and without a neutral density filter in front of one eye (Pulfrich Phenomenon). The neutral density filter affects the luminance and introduces a time delay in processing the retinal image (Wilson and Anstis, 1969; Reynaud and Hess, 2017), and the pendulum is perceived to move in an elliptical path.

As per our proposed model, the change in temporal information affects the interaction between the spatial and temporal information, which modulates the perception of the position of the moving pendulum. During perceiving the moving object and Pulfrich illusion, the same visual area V5 is active, which validates that both the perception of moving object and Pulfrich illusion involve the interaction between the spatial and temporal information. Furthermore, we verified that the area V5 is where the visual-spatial information and temporal information interact, by performing the MRI tractography investigations. Thence we found the neural tracts between the area V5 and relevant brain regions, thus linking the areas of visual-spatial perception and temporal perception. The centrality analysis of the network (considering the brain regions as nodes and neural tracts as the connection between them) yields that area V5 is the most important node.

3.7.3 Neuronal Framework

The neurons in the area V5 are tuned to the particular speed of the moving object (Perrone and Thiele, 2001, 2002). We elucidated that spatial and temporal information interaction should occur at the visual area V5. We devised a mathematical model based on the Lotka-Volterra system to quantify the interaction between the visual-spatial and temporal

perception mediated by Acetylcholine and Dopamine neurotransmitters at area V5. In our model, the interaction parameter (m) denotes the level of the interaction. For m=1, we obtained the oscillatory nature of the Acetylcholine and Dopamine concentration with a phase difference of 90 degrees. The phase difference decreases, and the period of oscillatory concentration increases as the interaction parameter (m) increases. Using the concepts of vector algebra, we represented the spatial and temporal perception as orthogonal vectors. Further mathematical analysis yielded that the spatiotemporal perception of moving objects can be represented as a complex number (real part: spatial information and imaginary part: temporal information). The 90° phase difference between the Acetylcholine and Dopamine concentration is denoted by the $j\ (=\ \sqrt{-1})$ in complex number representation. We showed that the orthogonal components of the spatial information and temporal information interact. Therefore the phase difference decreases as the interaction parameter (m) decreases and, thus, there is reduction in the interaction between the spatial and temporal information.

Further, we delineated that the interaction between Acetylcholine and Dopamine (mathematically denoted by the interaction parameter) modifies the spatiotemporal receptive field properties of the complex cell at the area V5. Due to this, the complex cell will now be tuned for another speed. This change in the tuned speed will be minimal and insignificant for lower speeds but gradually increase and become significant as the speed of the moving object increase. Thus, we could interpret that the interaction parameter (m) is proportional to the speed of the moving object (P) because the interaction parameter affects the interaction between the Acetylcholine and Dopamine, which will manifest as modulation in the perception of the moving object, similar to how the speed of the object modulates the perception.

3.7.4 General Significance and Applicability:

It is interesting to note that blind wounded soldiers having an injury to the primary visual cortex can perceive motion without perceiving the properties like color and shape of the moving stimulus (Riddoch, 1917). This suggests that even though the transmission of visual information from the primary visual cortex to area V5 is impaired, area MT/V5 *per se* is active and receives information from the other brain regions while perceiving moving objects (Zeki and Ffytche, 1998). Hence we can conclude that spatial and temporal information streams from brain regions other than the primary visual cortex may meet at area MT/V5. Furthermore, these information streams from different brain regions may carry information extracted from the other sensory systems. Therefore, area MT/V5 may act as a spatio-temporal information interaction point for other sensory systems apart from vision. Indeed, experimental research studies also point to a similar direction regarding visual, auditory, and tactile motion processing (Krug, 2004; Poirier et al., 2005; Amemiya et al., 2017). Our results imply that the proposed approach to understanding the modulation of the perception due to the dynamics of the causal states of an event may be generalized to different sensory systems. In principle, cerebral area V5 processes information from other sensory systems too (Krug, 2004; Poirier et al., 2005; Amemiya et al., 2017); hence, our mathematical framework and analysis may be scalable and applicable to the more wide-ranging nature of area V5, which may be useful to understand the general principle of brain function (Zeki, 2015). Furthermore, our model can be helpful when a human operator works in an environment consisting of very fast-moving objects (at high speed, the perception of moving object is modulated significantly and cause errors in judgment). A perceptual error warning system based on our mathematical model can be used to issue an alerting signal to a human operator in cases like the pilot of a fighter jet or over-speeding driver of a vehicle.